Sanaye, Sepehr; Hosseini, Salahadin

Article

Prediction of blade life cycle for an industrial gas turbine at off-design conditions by applying thermodynamics, turbo-machinery and artificial neural network models

Energy Reports

Provided in Cooperation with:
Elsevier

Suggested Citation: Sanaye, Sepehr; Hosseini, Salahadin (2020) : Prediction of blade life cycle for an industrial gas turbine at off-design conditions by applying thermodynamics, turbo-machinery and artificial neural network models, Energy Reports, ISSN 2352-4847, Elsevier, Amsterdam, Vol. 6, pp. 1268-1285,
https://doi.org/10.1016/j.egyr.2020.05.008

This Version is available at:
https://hdl.handle.net/10419/244119

Energy Reports 6 (2020) 1268–1285

Contents lists available at ScienceDirect

Energy Reports

journal homepage: www.elsevier.com/locate/egyr

Research Paper

Prediction of blade life cycle for an industrial gas turbine at off-design conditions by applying thermodynamics, turbo-machinery and artificial neural network models

Sepehr Sanaye *, Salahadin Hosseini

Energy Systems Improvement Laboratory, Mechanical Engineering Department., Iran University of Science and Technology, Iran

ARTICLE INFO

Article history:
Received 23 October 2019
Received in revised form 27 January 2020
Accepted 10 May 2020
Available online xxxx

Keywords:
Industrial gas turbine
Blade life cycle
Larson–Miller method
Neural Network

ABSTRACT

A novel method for estimating the rotor blade life cycle of an industrial gas turbine (GT) by the use of artificial Neural Network is proposed in this paper At the first step the blade life cycle is obtained by the use of Larson–Miller method which uses output results of GT performance modeling and blade thermal-mechanical data. Then results of rotor blade life cycle analysis by the above method are compared with results of stress factor curve (which is provided by manufacturers). Comparison of results revealed an average difference value of 9.7 % between blade life cycle estimation by two above mentioned methods. In the next step, by input data such as mass flow rate, temperature and pressure of hot flue gas, the output data such as blade cooling air and turbine shaft rotational speed are obtained from GT modeling. Then blade life cycle are also obtained by Larson–Miller method for 811 sample points of GT operating conditions for various ambient temperatures and load ratios. These data are used for neural network training. Results show that life cycle estimated values by neural network method in comparison with life cycle estimated values by Larson–Miller method, had about 4.8% error value in maximum (with 10-4 as mean square error, MSE). Finally, by the use of neural network method, the effects of gas turbine operating and health conditions (at various ambient temperatures, GT load ratios and compressor fouling levels) on blade life cycle are investigated. If we expect to get the nominal power output of clean blade at ISO ambient condition, in ambient temperature range of 15 to 45 °C, the GG turbine first rotor blade life cycle reduces from 4.85 to 0.07 and in the range of 0 to 7% compressor fouling, turbine blade life cycle reduces from 4.85 to 0.68 years.

1. Introduction

Industrial gas turbines play a key role in process plants (as mechanical driver for compressors or pumps) and in distributed generation power plans (as turbo-generator). Thus, the reliability and availability of these machines are of vital importance for the plant owners. The engine reliability and availability are directly related to the engine working hours (ISO 3977-9 Internal Standard, 1999) which mainly depends on the engine hot section part life cycle. Due to this fact, even online estimation of engine part life cycle is required for making appropriate control and operation decisions as well as to perform condition based inspection and maintenance.

Tahan et al. (2017) reviewed different methods for prognostic and condition based operation and maintenance of gas turbine. They mentioned that the intelligent methods such as Artificial Neural Network and Genetic algorithm are among useful methods for gas turbine fault detection, fault isolation and developing condition based maintenance system. Li and Nilkitsaranont (2009) proposed a novel method to estimate the gas turbine remaining useful life before major overhaul for performing condition based maintenance instead of time-scheduled maintenance. The method was based on combined linear and quadratic regression methods to fit a model to the historical engine operating data (which included different engine health and operating conditions) for computing the gas turbine remaining life cycle.

Furthermore, in order to apply the method of prognostic and condition based inspection and maintenance of gas turbine; models are developed for estimating the life cycle of the engine hot section parts based on the engine operating conditions. Ghafir et al. (2014) also used Neural Network Algorithm for proposing an improved life cycle estimation model for turbine blade of an aero-engine. They applied engine off design modeling results for thermal analysis of blades by conjugate heat transfer method and life cycle analysis by the use of Larson–Miller method. The results in the next step are used for training the Neural Network Algorithm.

* Correspondence to: Iran University of Science and Technology, Narmak, Tehran 16844, Iran.
E-mail address: sepehr@iust.ac.ir (S. Sanaye).

https://doi.org/10.1016/j.egyr.2020.05.008

Nomenclature

C	Velocity (m/s)
CFD	Computational fluid dynamic
Cp	Specific heat (kJ/kg °K)
Eff	Efficiency
EOH	Equivalent operating hours
EOC	Equivalent operating cycles
FAR	Fuel air ratio
GG	Gas Generator (rpm)
GC	Gas compressor
H	Engine real operating hours (h)
IGV	Inlet guide vane
LHV	Lower heating value (kJ/kg)
LMP	Larson–Miller Parameter
Ma	Mach number
M	Non-dimensional corrected inlet mass flow rate
$\dot{m}$	Mass flow rate (kg/s)
MSE	Mean square error
N	Non-dimensional corrected shaft speed
NGG	Gas generator speed (rpm)
NGV	Nozzle Guide Vane
NPT	Power turbine speed (rpm)
Ns	Number of samples
P	Pressure (bar)
PR	Pressure ratio
PT	Power turbine
R	Universal gas constant (J/mole K)
T	Temperature (K)
TIT	Turbine inlet temperature (K)
TET	Turbine exit temperature (K)
t_f	Turbine blade life (years)
U	Rotor tangential velocity
xj	Neural Network input parameter
Y	Momentum loss parameter
y	Mole fraction
y_k	Neural Network output parameter
Znorm	Neural Network predicted target

Greek letters

Φ	Cooling effectiveness
η	Efficiency (%)
β	Metal angle
β_s	Beta line slop
α	Absolute flow angle
ρ	Density (kg/m^3)
ω	Rotational speed (rad/s)
π	Corrected pressure ratio
γ	Specific heat ratio
Γ	Compressor fouling percent
τ_x	Stress factor
τ_f	Fuel factor
τ_w	Water injection factor

Subscripts

A	Axial
Av	Average
B	Blade
C	Coolant
Comb	Combustion chamber
Comp	Compressor
Corr	Corrected
Ex	Exit
F	Fuel
G	Gas
GC	Gas compressor
In	Inlet
Isent	Isentropic
M	Metal
Max	Maximum
Min	Minimum
Pt	Power turbine
Ref	Reference
S	Static
Sh	Shaft
Stoich	Stoichiometric
Th	Thermal
Tot	Total
Turb	Turbine

In another research by the same authors (Abdul Ghafir et al., 2010), a model named Creep Factor (CF) is proposed which could estimate the blade life cycle based on the deviation of GT operating conditions from those at the design point. Parthasarathy et al. (2008) also used Neural Network modeling for estimation of thermal stress as well as the maximum temperature in turbine blades by the use of turbine rotating shaft speed and inlet hot gas temperatures. Zaretsky et al. (2012) proposed a relation for fast estimation of blade life cycle based on using real data obtained from an aero-engine in various operating conditions. With gathering the real engine data, they categorized different reasons of aircraft engine turbine blade failures such as thermal-mechanical fatigue and oxidation/erosion. Then they formulated the turbine blade life cycle from classified field data. Vaezi and Soleymani (2009) computed the creep life of an industrial gas turbine via experimental and analytical (by the use of Larson–Miller formula) methods. They proved that Larson–Miller method has good accuracy in predicting the life cycle of a turbine blade (which is made from INC 738 super alloy).

Wood (2000) reviewed different methods and technologies for measuring the remaining life of gas turbine components. These methods were non-destructive (such as detecting damages and cracks using radiography test of specific components) examinations, destructive evaluation and to compute the remaining life cycle. The third investigated method requires the detailed modeling of heat transfer and stress distribution in the turbine blade. They justified that the creep is the main cause of life cycle reduction in hot section parts of industrial gas turbines operating at base and peak load conditions (Wood, 2000). Marahleh et al. (2006) used the stress rapture tests for predicting the remaining life cycle for turbine blade of an industrial gas turbine. The test specimens were prepared from the first stage turbine blade of an industrial gas turbine (which had been in service from 30 000 to 80 000 h) and all tests were performed by applying 400 to 600 MPa tensile stresses in 850 °C of test temperature. Finally the Larson–Miller parameter was used to correlate the test results to the actual operating condition of the GT. Also, Mino et al. (2001) proposed a method to predict the turbine blade life cycle of an aero derivative gas turbine by measuring the turbine blade

elongation during engine maintenance. This proposed method could be categorized as a nondestructive testing.

Researchers also investigated the effect of different engine performance parameters on the turbine blade life cycle using blade life analysis models.

Hay and Taylor (1984) used analytical correlations for estimating the turbine blade metal temperature and life cycle and investigated the effect of turbine blade cooling air temperature reduction on the turbine blade life cycle and engine thermal efficiency. They found that reducing the turbine cooling air temperature can reduce the cooling air mass flow rate up to 40% (without sacrificing the turbine blade life cycle) and could also increase the engine thermal efficiency. Eshati et al. (2013) proposed an analytical model to investigate the effect of water–air ratio on an industrial gas turbine blade life cycle in case of high water content in compressor intake air. This condition occurs when GT is working in a humid climate or when a water spray in compressor intake is used for compressor inlet air cooling for increasing the power output. The model is based on the turbine blade metal temperature estimation (by convective and conductive heat transfer modeling and assuming a simplified geometry for the turbine blade) and the use of Larson–Miller creep model for turbine blade life cycle estimation. The use of Larson–Miller model in this reference was due to considering creep as the dominant mechanism for the reduction of life cycle for industrial gas turbines working at high load ratios. In the above mentioned references the developed models for estimating the turbine blade life cycle is based on the engine performance parameters such as turbine exit temperature, engine load ratio (the ratio of power output at a certain ambient condition to the GT nominal power output) and engine operating conditions such as ambient temperature. However, a model is developed here to estimate the industrial gas turbine rotor blade life cycle as a function of effective parameters on the turbine blade heat transfer and thermo-mechanical stresses. This model provides an accurate assessment of turbine blade life cycle in different engine operating and health conditions. Thus, a procedure for estimating an industrial gas turbine rotor blade life cycle is proposed. This procedure is based on blade thermal analysis (by conjugate heat transfer method) besides applying Artificial Neural Network method. The effects of ambient air temperatures, load ratios and compressor fouling percent on the turbine blade life cycle are used to train an artificial neural network model. Since the operation of GT at base and peak loads is associated with high turbine inlet temperatures and huge centrifugal stresses in the turbine blade, the main focus of this paper is blade life cycle analysis in these conditions.

The novelty of the proposed procedure for the life cycle estimation is summarized in the following:

- Developing a trained neural network model for estimating the turbine blade life cycle as a function of parameters which affect the blade metal temperature and thermo-mechanical stresses. These parameters are turbine inlet gas temperatures and cooling air pressures, temperatures and mass flow rates together with turbine shaft rotational speed which are computed using gas turbine performance modeling.
- Investigating the effect of variable geometry turbine and compressor (variable NGV and IGV angles) on the turbine blade life cycle by the use of GT cycle modeling and the trained Neural Network output.
- Investigating the effects of engine operating conditions (such as different ambient temperatures, various load ratios or GT power output, and different levels of compressor fouling) on turbine blade life cycle.

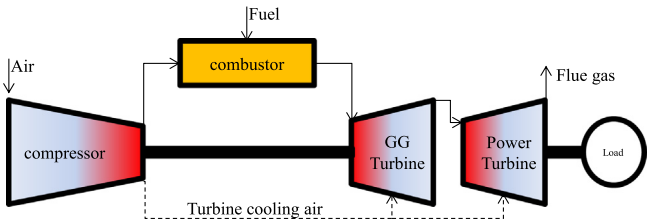

Fig. 1. Twin shaft gas turbine.

The developed model is able to take into account engine geometrical parameters (various IGV and NGV angles) and different engine health conditions (various compressor fouling percent) for estimating the turbine blade life cycle which is a novel approach in this field.

2. Gas turbine performance modeling

The twin shaft gas turbine (as shown at Fig. 1) performance modeling is developed based on thermodynamic matching method and using the compressor and turbine characteristics data which are provided in Rashidzadeh et al. (2015).

Therefore as the first step, mass and energy balance equations for the gas turbine components (such as compressor, combustor and 4 turbine stages) are solved by iterative Newton–Raphson method (Deuflhard, 1974; Ben-Israel, 1966). The method starts with using initial values for parameters. These values then become modified and reach the final values of parameters which satisfy the system of conservation equations.

The unknown parameters for simulating the twin shaft gas turbine are:

- Gas turbine cooling streams (five parameters for five streams)
- Compressor pressure ratio (one parameter)
- Gas generator(GG) & Power turbine(PT) pressure ratios (four parameters for two stages of GG and two stages of PT)
- GG turbine rotating speed (one parameter)
- PT turbine rotating speed (one parameter) in case of modeling the GT as mechanical driver.
- fuel mass flow rate (one parameter)

In each iteration compressor and turbine corrected inlet mass flow rates and the isentropic efficiency are computed by fitting a third order polynomial to the characteristic maps of compressor and turbine in form of the following equations:

$$\dot{M}_{in}(\pi, N) = c_1(N)\pi^3 + c_2(N)\pi^2 + c_3(N)\pi + c_4(N) \quad (1)$$

$$c_i = c_{i1}N^3 + c_{i2}N^2 + c_{i3}N + c_{i4} \quad (2)$$

$$\eta_{is}(\pi, N) = b_1(N)\pi^3 + b_2(N)\pi^2 + b_3(N)\pi + b_4(N) \quad (3)$$

$$b_i = b_{i1}N^3 + b_{i2}N^2 + b_{i3}N + b_{i4} \quad (4)$$

For compressor map π is the compressor corrected pressure ratio (PR/PR_{design}) and N is compressor non-dimensional corrected rotating shaft speed (which is equal to $N_{GG}/\sqrt{T_0}/\left(N_{GG}/\sqrt{T_0}\right)_{design}$ and $\dot{M}$ is compressor non-dimensional corrected inlet mass flow rate (which is equal to $\frac{\dot{m}_{in,comp}\times\sqrt{T_{in,comp}}}{P_{in,comp}}/\left(\frac{\dot{m}_{in,comp}\times\sqrt{T_{in,comp}}}{P_{in,comp}}\right)_{design}$).

Furthermore, for GG and PT turbine maps, π is the turbine stage corrected pressure ratio (PR/PR_{design}) and N is turbine non-dimensional corrected rotating shaft speed (which is equal to $N_{GG}/\sqrt{T_{in,GG}}/\left(N_{GG}/\sqrt{T_{in,GG}}\right)_{design}$ for GG and $N_{PT}\Big/\sqrt{T_{in,pt}}\Big/$

$\left(N_{PT}\Big/\sqrt{T_{in,pt}}\right)_{design}$ for PT turbine). Also, $\dot{M}$ is turbine stage non-dimensional corrected inlet mass flow rate (which is equal to $\frac{\dot{m}_{in,turb}\times\sqrt{T_{in,turb}}}{P_{in,turb}}\Big/\left(\frac{\dot{m}_{in,turb}\times\sqrt{T_{in,turb}}}{P_{in,turb}}\right)_{design}$). Moreover, $c_{i,j}$, $b_{i,j}$ are coefficients of polynomial fitting to the compressor or turbine characteristic maps (which are obtained by fitting third order polynomials to compressor and turbine maps).

After computing inlet mass flow rate ($\dot{m}$) and isentropic efficiency (η_{is}) with initial values of N and π, the compressor exit temperature, $T_{out,comp}$, compressor discharge pressure $P_{out,comp}$ and compressor power consumption is computed from following equations:

$$T_{ex,comp} = T_{in,comp}\left[1+\frac{1}{\eta_{comp}}\left(PR_{comp}^{\frac{\gamma-1}{\gamma}}-1\right)\right] \tag{5}$$

$$P_{ex,comp} = P_{in,comp}\times PR_{comp} \tag{6}$$

$$W_{comp} = \dot{m}_{in,comp}\times C_{p,a}\times\left(T_{out,comp}-T_{in,comp}\right) \tag{7}$$

Also, each turbine stage exit temperature, $T_{out,turb}$, exit pressure $P_{out,turb}$ and turbine power output W_{turb} are computed by the use of Eqs. (8) to (10):

$$T_{out,turb} = T_{in,turb}\left(1-\eta_{turb}\left[1-PR_{turb}^{\frac{1-\gamma}{\gamma}}\right]\right) \tag{8}$$

$$P_{out,turb} = P_{in,turb}/PR_{turb} \tag{9}$$

$$W_{turb} = \dot{m}_{in,turb}\times C_{p,g}\times\left(T_{in,turb}-T_{out,turb}\right) \tag{10}$$

The variable geometry turbine (variable NGV angle) and compressor (variable IGV angle) are entered in the GT modeling code using linear map scaling method. The detail of this method is presented in Appendix A. Furthermore, power turbine shaft rotating speed is fixed when PT is connected to a generator. In case of using turbo-shaft as mechanical driver (such as gas compressor in natural gas transportation pipeline), PT shaft speed should be estimated. The details of gas compressor modeling and estimation of N_{PT} are covered in Appendix B.

It should be mentioned that for cooling turbine blades in our studied turbo-shaft, air is extracted from the end of compressor (Fig. 1). The cooling air flows through turbine blade internal passages which is called internal convective cooling method (Sanjay et al., 2009). Coolant mass flow rates for each turbine row is computed using the method proposed in Refs. El-Masri (1988) and Kim et al. (1996). According to this method, the cooling air mass flow rates at various engine operating ranges (all off design conditions such as various ambient conditions, part loads and compressor fouling levels) can be estimated using Eq. (11).

$$M_c = K_c P_{comp}\sqrt{\frac{2\left(1-{}^{P_{turb}}/_{P_{comp}}\right)}{R\times T_{comp}}} \tag{11}$$

T_{comp}, P_{comp} and P_{turb} in Eq. (11) are total temperature and total pressure values for cooling stream exit from compressor and cooling stream inlet into the turbine. Also, K_c is turbine cooling path flow coefficient which is computed based on the maximum temperature tolerable by the turbine blade metal by the use of relations given in Ref. El-Masri (1988).

The studied engine as is shown in Fig. 1 has a Gas Generator Turbine (GG) and a Power Turbine (PT). Each turbine has two stages and each stage includes a stator and a rotor blade row. Both GG turbine stages and the first PT turbine stage are cooled by the use of air extracted from the compressor discharge. Thus power output, hot gas mass flow rate, temperature and pressure in each turbine stage are computed by the effect of mixing hot gases with stator and rotor cooling air. This is performed by the method proposed by Refs. El-Masri (1988) and Camporeale et al. (2006). Thus to compute each turbine stage power output, and for each exhaust mass flow rate, temperature and pressure, the effect of mixing hot gases with stator and rotor cooling air is modeled using the method proposed in Refs. El-Masri (1988) and Camporeale et al. (2006).

The flowchart in Fig. 2 shows the details of computation procedure in each turbine stage. Fig. 2 shows modeling procedure of flow in turbine rotor and stator which is performed by mixing the main hot gas stream with cooling air in both stator and rotor besides an expansion process in a turbine stage. This process results in the hot gas main stream enthalpy reduction and pressure drop. The mixing control volume outlet pressure and enthalpy are computed using the following equations:

$$h_{out} = \frac{\dot{m}_{\text{cooling air}}\times h_{\text{cooling air}}+\dot{m}_{\text{hot gas}}\times h_{\text{hot gas}}}{\left(\dot{m}_{\text{cooling air}}+\dot{m}_{\text{hot gas}}\right)} \tag{12}$$

$$P_{out} = P_{in}.\left[1-\frac{\dot{m}_{\text{cooling air}}}{\dot{m}_{\text{hot gas}}}(1-Y).\gamma.Ma^2\right] \tag{13}$$

where Ma is Mach number computed at the blade throat section. This section is the gas flow frontal area between two turbine blades at the blade exit (or blade trailing edge). Y is the momentum loss parameter (Camporeale et al., 2006):

$$Y = \gamma Ma^2/2\left(1+\frac{\gamma-1}{2}Ma^2\right)^{\frac{\gamma}{\gamma-1}} \tag{14}$$

Thus the effect of turbine cooling air on mass flow rate, temperature and pressure of hot gas streams as well as various turbine stage power output are taken into account.

Combustion chamber exit temperature and the flue gas composition are computed via the energy balance by the use of initial value for fuel mass flow rate as below:

$$\dot{m}_{air}h_{in,comb}+\dot{m}_{fuel}LHV = \dot{m}_g h_{in,turb}+(1-\eta_{comb})\dot{m}_{fuel}LHV \tag{15}$$

$$\frac{P_{ex,comb}}{P_{in,comb}} = \left(1-\Delta P_{comb}\big/100\right) \tag{16}$$

The combustion reaction equation in combustor is:

$$\lambda C_{x1}H_{y1}+\left(x_{O_2}O_2+x_{N_2}N_2+x_{H_2O}H_2O+x_{CO_2}CO_2\right)\rightarrow y_{CO_2}CO_2 +y_{N_2}N_2+y_{O_2}O_2+y_{H_2O}H_2O+y_{NO}NO+y_{CO}CO \tag{17}$$

$$\begin{aligned} y_{CO_2} &= \left(\lambda\times x_1+x_{CO_2}-y_{CO}\right)\\ y_{N_2} &= x_{N_2}-y_{NO}\\ y_{H_2O} &= x_{H_2O}+\frac{\lambda\times y_1}{2}\\ y_{O_2} &= x_{O_2}-\lambda\times x_1-\frac{\lambda\times y_1}{4}-\frac{y_{CO}}{2}-\frac{y_{NO}}{2} \end{aligned} \tag{18}$$

In above equations λ is combustion equivalent ratio which is defined as actual fuel to air ratio to stoichiometric fuel to air ratio:

$$\lambda = \frac{FA_{actual}}{FA_{\text{stoich}}} \tag{19}$$

The combustion chamber pressure drop is computed using following correlations provided at Rashidzadeh et al. (2015) for the studied gas turbine.

$$\Delta P_{comb} = 0.000404\times\left(\frac{\dot{m}_{in,comb}\sqrt{T_{in,comb}}}{P_{in,comb}}\right)^2+0.00758 \times\frac{\dot{m}_{in,comb}\sqrt{T_{in,comb}}}{P_{in,comb}} \tag{20}$$

The following thermodynamic relations for computing the air and combustion gas properties were used from correlations provided in Ref. VanWylen et al. (1998).

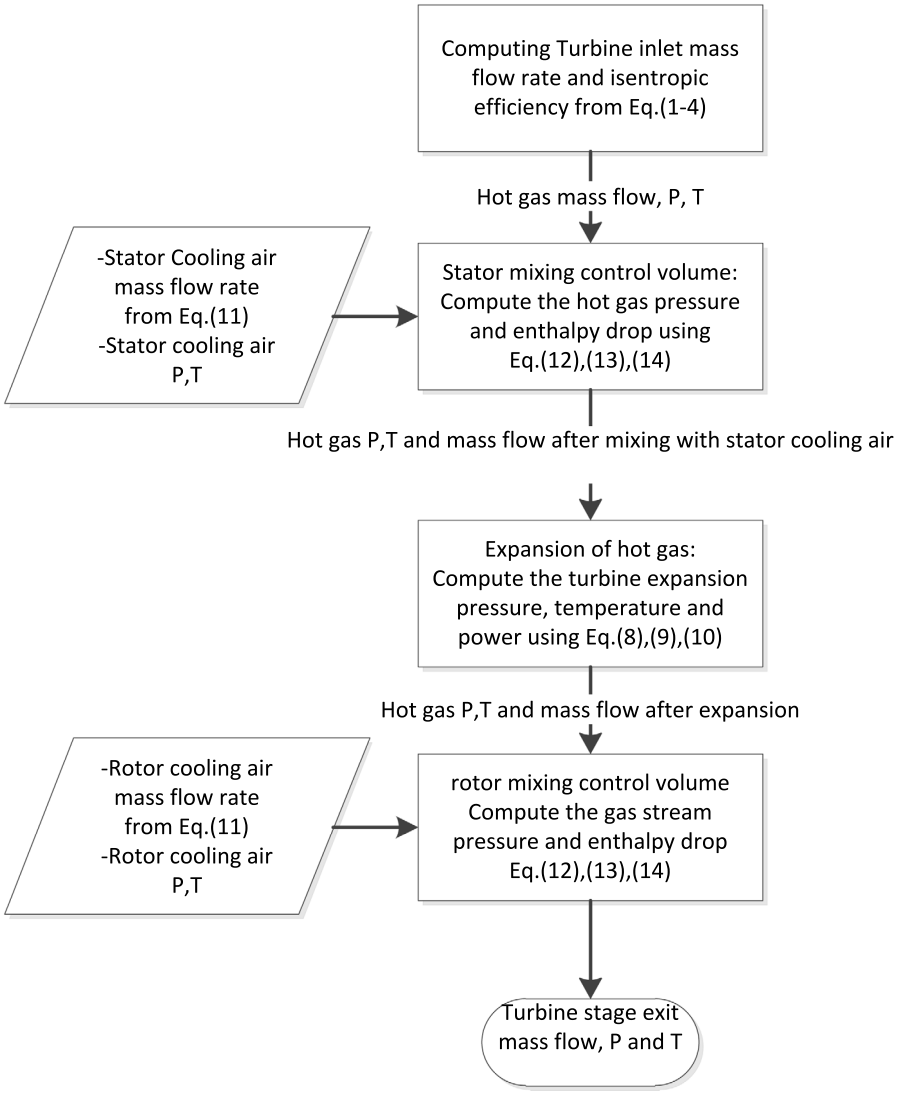

Fig. 2. The procedure of flow modeling in turbine with cooling of both stator and rotor blades.

For air:

$$C_{p,air}(T) = 1.04841 - \left(\frac{3.8371T}{10^4}\right) + \left(\frac{9.4537T^2}{10^7}\right) - \left(\frac{5.49031T^3}{10^{10}}\right) + \left(\frac{7.9298T^4}{10^{14}}\right) \quad (21)$$

For combustion gases:

$$C_{p,gas}(T) = \sum y_i C_{P_i} \quad (22)$$

In Eq. (22) y_i is the mole fraction of species in combustion product which are computed by Eq. (18).

Compressor fouling

Compressor fouling, changes the compressor blade geometry and reduces the compressor isentropic efficiency as well as reducing inlet mass flow rate and pressure ratio (Fouflias et al., 2010). These drawbacks affect the engine performance and life cycle of components as well. To model the compressor fouling, the compressor characteristic map (corrected inlet mass flow rate, isentropic efficiency and pressure ratio) are modified for a specified percent of compressor fouling based on the method presented in Ref. Mohammadi and Montazeri-Gh (2014).

In this method, the change in compressor air mass flow rate at the fouled condition in comparison with that for the clean condition is equal to the compressor fouling percent. Furthermore, the change of compressor isentropic efficiency at the fouled condition in comparison with that for the clean condition is one third of the fouling percent. This fact is justified by the use of experimental data and turbo-machinery analysis as is described in Ref. Mohammadi and Montazeri-Gh (2014). Thus the reduced compressor inlet mass flow rate due to existing fouling can be related to $\dot{m}_{in,comp}$, at clean condition with Eq. (23) and the compressor isentropic efficiency can be related to its value at clean condition, $\eta_{is,comp}$, with Eq. (24).

$$\dot{m}_{in,comp,f} = \dot{m}_{in,comp} \times \left(1 - \frac{\Gamma_C}{100}\right) \quad (23)$$

$$\eta_{is,comp,f} = \eta_{is,comp} \times \left(1 - \frac{\Gamma_C}{3 \times 100}\right) \quad (24)$$

Γ_C, is the compressor fouling in percent (with a positive value). $\dot{m}_{in,comp,f}$, and $\eta_{is,comp,f}$ are compressor inlet mass flow and isentropic efficiency in the fouled condition respectively. As Eq. (23) explains, the value of Γ_C in percent, shows the percent of reduction in air inlet mass flow rate of compressor at the fouled condition.

The reduction in compressor pressure ratio PR (due to fouling) can be also expressed by the use of fouling percent, Beta line

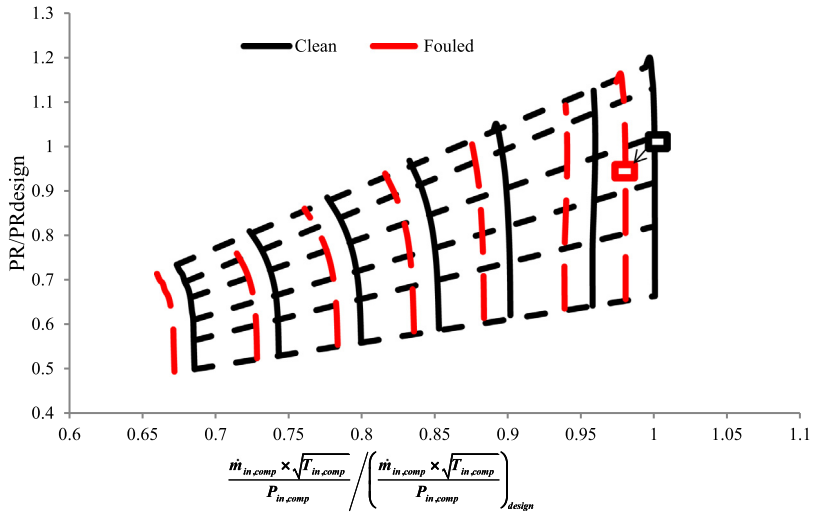

Fig. 3. Compressor map at clean and fouled conditions.

slop (as shown in Fig. 3) and the compression ratio for the clean compressor, PR $_{comp}$, at each specific location in the compressor map (Eq. (25)).

$$PR_{comp,f} = PR_{comp} \times \left(1 - \frac{\Gamma_C \times \beta_s}{100}\right) \tag{25}$$

For example if the compressor fouling is 3% and the Beta line slop (β_s) is 0.8, the compressor pressure ratio reduction is 2.4%. Fig. 3 compares the compressor map in clean and fouled conditions. As per this figure, compressor fouling moves the compressor map toward lower non-dimensional corrected inlet mass flows and lower corrected pressure ratios.

3. Life cycle analysis

Only the first row blade of high pressure turbine (Gas Generator turbine of the studied industrial gas turbine) is selected for life cycle analysis by Refs. Abdul Ghafir et al. (2010), Eshati et al. (2013) and Eshati (2012). The first row blades are adjacent to the combustion chamber exit and are exposed to high temperature and pressure flue gases. Thus at these critical operating conditions the highest thermal and mechanical stresses exist for the first row of the HP turbine blade in comparison to other turbine parts such as stators and disks. It should be noted that the turbine stator blades are fixed without exposing to centrifugal stress. Furthermore, turbine disks are thick and back to back welded together, so they are not directly and fully exposed to the hot flue gases.

3.1. Gas turbine blade life cycle estimation by Larson–Miller method

Industrial gas turbines mostly operate at base and peak load conditions which associate with the high turbine inlet temperature together with the high mechanical stresses which are caused by shaft rotational speed. As is also justified in Refs. Wood (2000) and Eshati et al. (2013), the main reason of turbine blade life cycle reduction when GT is working at base and peak load conditions (load ratio equal to or greater than 100%) is creep. This is due to working the engine hot section parts at high thermal and mechanical stress conditions. Thus for modeling blade life cycle analysis, Larson–Miller method (Eq. (26)) is applied (Eshati, 2012). Larson–Miller is an accurate method for estimating the time of the creep failure which occurs as the result of simultaneous effect of mechanical and thermal stresses for different materials. The plot of Larson–Miller parameter (LMP) versus the total stress is named the creep curve which can be obtained from experimental data and are available for each specific material. LMP has an inverse relation with the total stress ($LMP\alpha\frac{1}{\sigma}$). Larson–Miller relation is shown in Eq. (26) (Eshati et al., 2013; Evans and Wilshire, 1993).

$$\log tf = \frac{LMP}{T_m} - C_{LMP} \tag{26}$$

Eq. (26) shows that the blade creep life cycle (t_f) is a function of blade metal temperature T_m and LMP value which is a function of total mechanical and thermal stresses. In this relation C_{LMP} is a constant parameter. The value of C_{LMP} can be obtained by creep test of super alloy specimens of gas turbine blade and can be selected as a fixed number (20) (Eshati et al., 2013).

Fig. 4 shows the procedure of estimating the blade creep life cycle. The procedure starts with creating 3D model of the blade in CAD software which is imported by ANSYS (which is software for stress analysis using finite element method). Then, the 3D model is discretized by using unstructured grids. By specifying input data such as density, thermal conductivity and by exerting boundary conditions, ANSYS computes the stress (total stress) distribution through the blade.

The followings boundary conditions are applied:

- The blade rotational speed creates centrifugal stresses inside the blade
- 3D metal temperature distribution throughout the blade may result in expansion and contraction as well as thermal stresses in some regions (Alizadeh et al., 2014).
- The pressure distribution on the blade surface and cooling air pressure inside the blade, result in mechanical stresses in the blade metal (Alizadeh et al., 2014).
- The blade is supported at root with free movement at tip.

After stress analysis, the creep life cycle is computed at each computation node using the computed total stress, stress-LMP curve and blade metal temperature by Eq. (26). The minimum amount of the creep life in the solution domain is taken to be the blade creep life. In this paper, the results of the flow and heat transfer analyses for the studied rotor blade life cycle is used from Ref. Alizadeh et al. (2014). In this reference, the blade heat transfer analysis is performed using conjugate heat transfer method. Thus, simultaneous solution of the fluid flow and convective heat transfer on the blade outside and inside surfaces as well as conduction heat transfer inside the blade metal are performed using CFD analysis.

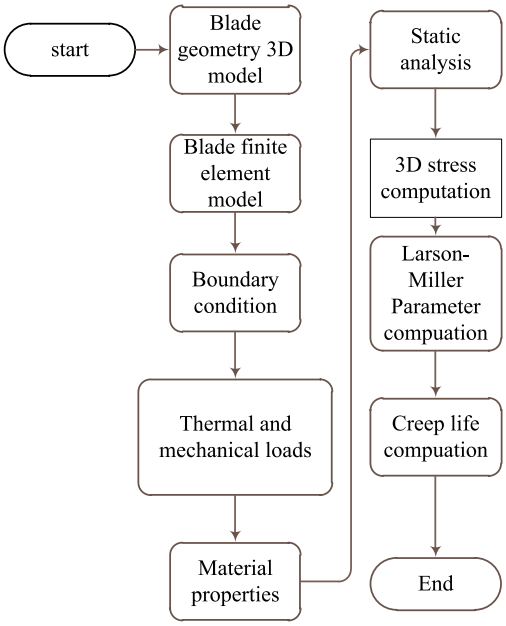

Fig. 4. Flow chart of rotor blade creep life cycle analysis.

For the above flow and thermal analyses, one stage of turbine (from the beginning of the stator entrance to the end of the first rotor blade exit) is modeled. The 3D flow domain is analyzed using unstructured grids and SST-kω two equations turbulence model is selected in ANSYS CFX. Turbine blade cooling air flow analysis is also performed by one dimensional flow modeling based on theories mentioned in Ref. Meitner (1990). The boundary conditions are stage inlet total pressure, total temperature, stage outlet static pressure, cooling passage inlet total pressure and total temperature, and rotor blade rotational speed. These data are extracted by the use of GT simulation program. Since the developed GT modeling code just computes the total gas properties such as total pressures and total temperatures, thus the stage outlet static pressure is computed by the use of stage exit mass flow rate and exit total pressure (which is computed from GT simulation program). The procedure for computing the static pressure at the rotor blade exit (or stage outlet) uses the following turbo machinery and thermodynamic relations:

$$\phi = \frac{C_a}{U} = \frac{C_a}{r\omega} \tag{27}$$

$$\tan\alpha_{out} = \tan\beta_{out} - \frac{1}{\phi} \tag{28}$$

$$C = \frac{C_a}{\cos(\alpha_{out})} = \frac{\dot{m}g + \dot{m}c}{\rho A_{out}\cos(\alpha_{out})} \tag{29}$$

where ϕ is the flow coefficient, C_a is the axial velocity of the flue gas at the stage rotor exit (Fig. 5), U is blade tangential velocity which is equal to rotor angular velocity (ω) multiplied by rotor radius (r), $\dot{m}g$ and $\dot{m}c$ are the flue gas and cooling air mass flow rate respectively. Moreover, α_{out} is the flow angle at the blade exit, β_{out} is the metal angle (Fig. 5), ρ and A are flue gas density and flow frontal area at the blade outlet. After computing the flow absolute velocity at the blade outlet, the flow Mach number and static pressure are computed by the use of Eqs. (30) and (31):

$$Ma = \frac{C}{\sqrt{\gamma RT}} \tag{30}$$

$$P_s = \frac{P_{tot}}{\left(1+\frac{\gamma-1}{2}Ma^2\right)^{\frac{\gamma}{\gamma-1}}} \tag{31}$$

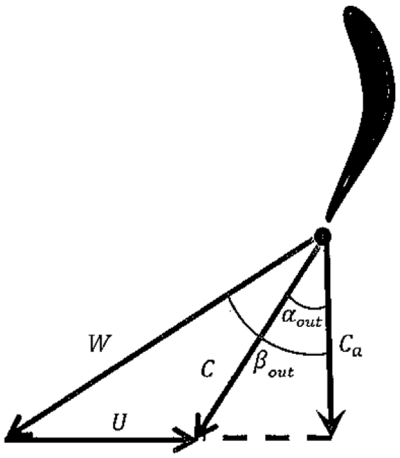

Fig. 5. Velocity triangle for turbine rotor blade.

Regarding input and output values of blade thermal analysis in Ref. Alizadeh et al. (2014), the following parameters are selected as effective parameters in GG turbine rotor blade life cycle:

- The hot flue gas total temperature, total pressure and mass flow rate (Tg, Pg, $\dot{m}g$) affect the flow Reynolds number and consequently change the Nusselt number and convective heat transfer coefficient on the blade airfoil surface.
- The cooling air total temperature, total pressure and mass flow rate (Tc, Pc, $\dot{m}g$) inside rotating blades affect the heat transfer parameters inside the blade cooling passages.
- Turbine shaft rotating speed (N_{GG})

Heat transfer coefficients at both blade outside and inside surfaces determine the blade metal temperature and affect the blade creep life cycle (Eshati et al., 2013). Furthermore, the temperature difference between the blade inside and outside surface creates thermo-mechanical stresses in the blade wall which affect the blade creep life (Eshati, 2012).

Thus the effective parameters for the rotor blade life cycle modeling are hot flue gas mass flow rate ($\dot{m}g$), temperature (Tg), pressure (Pg) and cooling air mass flow rate ($\dot{m}c$), temperature (Tc) and pressure (Pc) and also GG turbine shaft rotational speed (N_{GG}). It should be noted that the $\dot{m}g$, Tg, Pg, $\dot{m}c$, Tc, Pc, N_{GG} parameters are computed by GT modeling program (Rashidzadeh et al., 2015) and are used as input values for conjugate heat transfer modeling in CFD setup presented in Ref. Alizadeh et al. (2014). Blade conjugate heat transfer analysis is then used as boundary conditions for stress and life cycle analysis using finite element method. Thus the blade life cycle is assumed to be a function of $\dot{m}g$, Tg, Pg, $\dot{m}c$, Tc, Pc, N_{GG} parameters.

The above mentioned procedure for turbine blade heat transfer and life cycle analysis are very time consuming. However we require preparing a model for fast estimation of the turbine blade life cycle as a function of mentioned effective parameters. Thus after verification of results for life cycle analysis, the learning procedure for Artificial Neural Network is performed with various engine operating parameters (as input data) and then life cycle estimation (as output data).

3.2. Gas turbine blade life cycle estimation by artificial neural network

Artificial neural network is a suitable algorithm for investigating multi variable problems. This algorithm includes various parallel computations (processors) which speeds up the computation process and imitates the living organism neural system. The

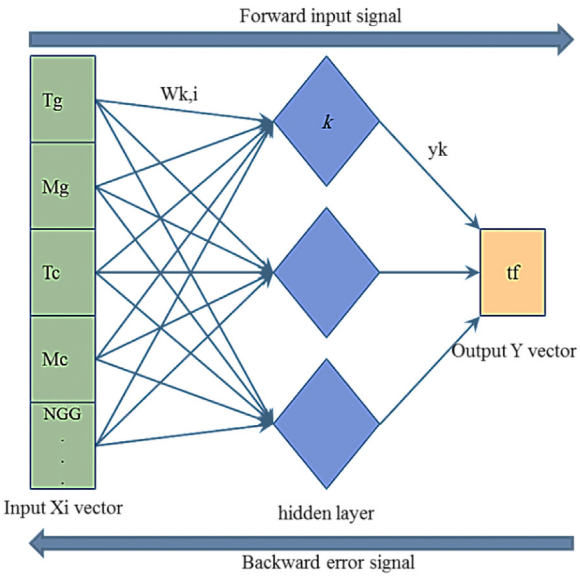

Fig. 6. Multi-layer feed forward back propagation artificial neural network (Rumelhart et al., 1985).

most commonly used type of neural network is Multi-layer Feed forward Back Propagation (MFBP) (Rumelhart et al., 1985).

As it is shown in Fig. 6, the algorithm includes two processors. The first processor sends input signals in forward direction and the second one sends the error signal (training error) in backward direction. As Fig. 6 shows, x, w, b and y parameters are inputs, synapse weight, bias and output signals respectively. The kth output in MFBP algorithm can be computed with relation 32.

$$y_k = \varphi_k\left(\sum_{j=1}^{n}\left(w_{k,j}x_j + b_k\right)\right) \tag{32}$$

In Eq. (32) φ is neuron activation function that controls the variation domain of neural network output signals and also gives the algorithm a nonlinear behavior. There are three types of the activation functions including Threshold function, Piecewise-Linear Function and Sigmoid Function (Haykin, 2001). Also Wk in Eq. (32) is synapse weights that link the output values to input values.

Artificial neural network training

Neural network training is an iterative process that adjusts the synapse weights to reach the intended outputs using specified input signals. In this paper the turbine blade life cycle has been computed for various amounts of effective parameters ($\dot{m}g$, Tg, Pg, $\dot{m}c$, Tc, Pc, N_{GG}). For this purpose, the neural network is trained. The input parameters for neural network training (X_j's in Fig. 6) are ($\dot{m}g$, Tg, Pg, $\dot{m}c$, Tc, Pc, N_{GG}) and output parameters (Y_j's in Fig. 6) is the turbine rotor blade life cycle (t_f in Eq. (26)) which is obtained from finite element analysis. During the training, validating and testing processes, the amount of the Mean Square Error (MSE) was computed and monitored by the use of Eq. (33).

$$MSE = \frac{\sum_{i=1}^{N_s}\left(\hat{z}_{norm} - z_{norm}\right)^2}{N_s} \tag{33}$$

where N_s, $\hat{z}_{norm}$, represent the number of samples in each training, validation, and testing samples and the normalized predicted and targeted output, respectively. In neural network training, synapse weights are adjusted in an iterative process until the Mean Square Error (MSE) reduces to an acceptable tolerance. It should be noted that epoch is the number of steps that the neural network iterates until the MSE reaches to an acceptable tolerance. The neural network method updates the synapse weights at each epoch.

For reducing the numerical error during neural network training the input parameters ($\dot{m}g$, Tg, Pg, $\dot{m}c$, Tc, Pc, N_{GG}) are made non-dimensional and normalized by dividing by their corresponding values at GT design point. The design point values are GT modeling program output at ISO condition.

3.3. Gas turbine blade life cycle estimation by stress factor curve

There is another method for predicting the GT blade life cycle for an industrial gas turbine. This method is based on computing engine Equivalent Operating Hours (EOH) together with using engine stress factor curve. However, this method is just applicable for a specific engine configuration (such as specific IGV and NGV values) and GT clean health condition for which the proposed stress factor curve is given by engine manufacturer. The equivalent operating hours is presented in Eq. (34) (Nyberg, 0000).

$$EOH = \tau_x.\tau_f.\tau_w.H + 5 \times EOC \tag{34}$$

One may consider EOH as the blade life cycle at the engine design point. Where H is the real operating hours (or real life cycle t_f in Eq. (26)) and τ_x is the stress factor. EOH is proposed by the engine manufacturers for different engine loads as presented in Fig. 7 (Nyberg, 0000) for ISO conditions. Typical figures exist from other manufacturers.

In Eq. (34), τ_f, τ_w show the coefficients for fuel type and water injection respectively. In case of no water injection and with natural gas as fuel, τ_f, τ_w are equal to one (Nyberg, 0000). EOC in Eq. (34) represents the total number of starts and stops for the studied engine. In case of GT operating at base and peak loads and the stable operation for the studied engine, EOC can be ignored in comparison with other terms in Eq. (34) (Rinman, 0000).

By omitting EOC and considering τ_f, τ_w equal to one and a fixed value for EOH in Eq. (34) (as a specific life time is expected from a part), then $EOH = \left(\tau_x.t_f\right)_{design} = \tau_x.t_f$. Thus t_f, the turbine blade life cycle is estimated from $t_f = \frac{EOH}{\tau_x}$ for an off-design condition. Eq. (34) as well as EOH and τ_x parameters which are introduced here, can be applied in Section 5.1 for verification of blade life cycle estimation.

According to Fig. 7 for GT load ratios (the ratio of power output at a certain ambient condition to the GT nominal power output at ISO ambient conditions) equal or higher than 100% (base and peak load conditions), the stress factor (τ_x) increases dramatically and with considering a fixed value for EOH (with omitting EOC term and substituting one for τ_f, τ_w), H in Eq. (34) (which is t_f) decreases sharply (Eq. (34)).

This is due to increase of turbine inlet temperature as well as increase of turbine blade metal temperature in GT base and peak loads that activates the creep phenomena in the turbine blade as also reported in Ref. Wood (2000). However in GT load ratios lower than 100% the stress factor has no significant change and no severe change in turbine blade life cycle occurs. However, as ambient temperature increases, compressor inlet air mass flow rate and the power output of GT reduce. In this case if we expect to get the same power output as that value for ISO ambient condition, the creep phenomena activates and reduces the turbine blade life cycle. This occurs due to the fact that at high ambient temperatures and with lower air mass flow rate, the fuel to air ratio raises which results in increase turbine inlet and exit temperatures (TIT and TET).

Thus, the stress factor is better to be presented as a function of deviation in turbine exit temperature (TET) from its corresponding value at the design condition (TET–TET_design). In this way increasing TET, more than that for the design value (TET_design),

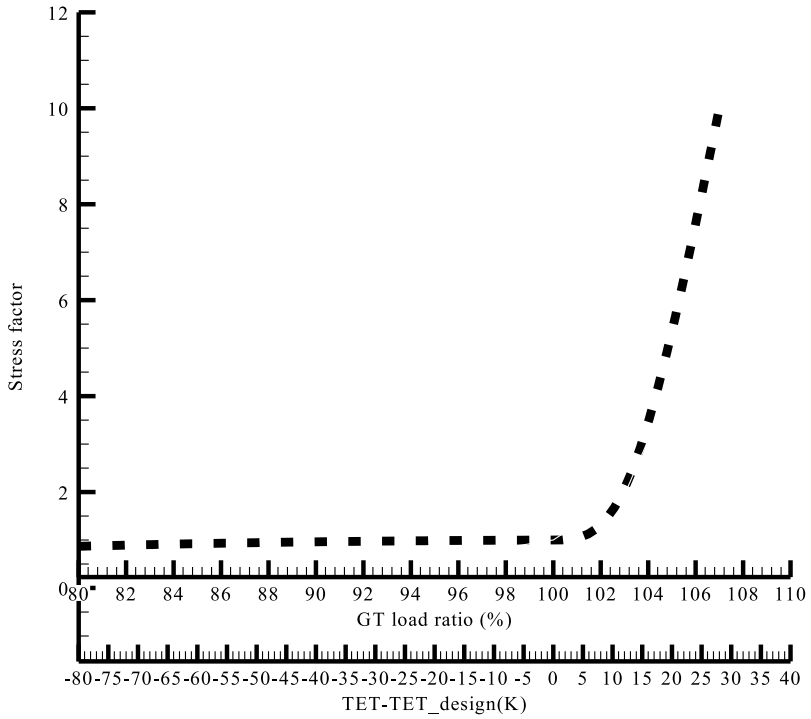

Fig. 7. SGT-600 gas turbine stress factor curve (Nyberg, 0000) at ISO condition and various partial loads.

means increasing the turbine inlet gas temperature more than that for the design value. This increases the stress factor (Fig. 7) which finally results in reducing the turbine blade life cycle.

Thus, if at each engine operating condition the turbine exit temperature is computed by the GT modeling code, with knowing difference of TET and TET_design, the stress factor (τ_x) can be computed from Fig. 7.

However, it should be noted that in case of change in compressor and turbine geometries (changing IGV and NGV angles for the engine upgrading or engine performance optimization) or change in engine health condition (such as compressor fouling which affect the compressor geometry), the rotor blade effective parameters also change and consequently the τ_x curve which is shown in Fig. 7, will not be applicable for the new IGV and NGV angles or faulty engine. Thus, for still being able to estimate the life cycle for all geometrical and fouling situations, a life estimating Neural Network model which works based on engine modeling results is developed here to be used for the entire range of ambient conditions, GT IGV and NGV angles and health conditions.

4. Case study

The studied turbine blade is the first rotor blade of SGT-600 gas turbine which is made from IN738 super alloy with tensile modulus of 148 GPa and Poisson ratio of 0.34. From SGT-600 maintenance plan (Siemens, 2006), the rotor blade design life cycle (or EOH in Eq. (34)) is 40 000 h or 4.56 years (each year is 8760 h).

GG turbine in this engine has two stages (i.e. two stators and two rotors, i.e., four rows), power turbine in this engine has also two stages (with four rows), and it also has an annular combustor with 18 burners. In the studied engine, the IGV angle varies from −8 to 36° and the NGV angle is fixed at 21° (NGV angle can be adjusted from 18 to 27° by opening the power turbine flange and changing the nozzle blade angle manually). The turbine exit temperature for the studied engine at the design point and ISO condition is 813 °K (Mohammadi and Montazeri-Gh, 2014).

Table 1
Input data for modeling validation at three different GT operating conditions.

	A	B	C
T_0 (°C)	10.6	19.8	29.6
P_0 (bar)	0.8	0.8	0.8
RH (%)	27.7	15.2	4.1
Pout_GC (bar)	77.6	70.9	72.4
Pin_GC (bar)	55.5	51.3	52.4
Tin_GC (°C)	32.1	31.9	31.4

As mentioned in Section 3.1, the turbine blade life cycle analysis is performed using CFD and finite element modeling for the GG turbine stage. The following steps are performed:

1—-The turbine stage geometry was created in CATIA mechanical drawing software. The intended solution domain was from stator inlet to rotor exit.

2—Blade-gen software sent geometry points of the above stage to Turbo-grid software for mesh generating of solution domain. The generated mesh was unstructured.

3—After sending the mesh structure to ANSYS CFX software, boundary conditions were also defined. Turbine stage boundary conditions were temperature, pressure at the flow inlet (i.e. stator inlet), rotor shaft speed and pressure at flow exit (i.e. rotor exit) and also cooling passage inlet total pressure and total temperature. The flow simulation was performed by the use of k-ε turbulent model.

The output results were checked for grid numbers from 1,200,000 to 1,800,000. Comparison of results showed that 1300,000 grids provided enough precision and uniqueness.

The combustion efficiency (in Eq. (15)) is considered to be 99%. Moreover, the natural gas fuel lower heating value is 46 760 kJ/kg. Moreover, in case of driving a gas compressor in natural gas transmission pipeline (turbo-compressor), the driven gas compressor has two stages with pressure ratio of 1.5.

Table 2
Comparison of output results for GT modeling (for input data given in Table 1) with experimental data.

GT operating condition (Table 1)	A			B			C		
	Site data	Modeling	Error (%)	Site data	Modeling	Error (%)	Site data	Modeling	Error (%)
Tex,comp (°C)	395.9	381.3	3.7	385.5	370.0	4.0	409.7	397.1	3.1
Pex,comp (bar)	11.6	11.2	3.6	10.2	9.7	4.7	10.3	10.0	2.6
NGG (rpm)	9961.4	9876.5	0.9	9661.0	9480.0	1.9	9850.0	9547.6	3.1
NPT (rpm)	7300.9	7347.2	0.6	7098.4	7098.4	0	7101.1	7101.1	0
TET (°C)	531.0	537.4	1.2	513.5	515.9	0.5	542.7	554.0	2.1
$\dot{m}_{in,GC}$ (MMD)	34.0	35.0	3.4	28.0	28.0	0	29.0	29.0	0
IGV (degree)	34	33	2.9	21	20	4.8	22	21	4.5
NGV (degree)	21	21	0	21	21	0	21	21	0
Heat flow (mJ/s)	51.4	54.6	6.3	43.8	44.6	1.7	44.6	47.4	6.4

5. Discussion and results

5.1. Model verification

5.1.1. Verification of GT modeling results

The modeling results for SGT-600 engine operating conditions at a gas pressure boosting station at southern region of Iran are compared with the corresponding experiment data. The modeling input data are presented in Table 1 for three different operating points named A, B, C.

Table 2 compares the modeling and experimental (measured) data at the site ambient condition. Table 2 shows that, the Maximum error (6.4 percent) occurs for the engine Input heating power (multiplying the fuel mass flow rate in kg/s, by fuel heating value in kJ/kg) at point C. This error either belongs to the modeling results (numerical errors in engine modeling) or the site fuel mass flow rate measurement. The average error for all parameters in this table is about 2.7 percent, thus the developed model for prediction of the GT performance here has an acceptable accuracy.

Fig. 8 compares the GT modeling results with 7.5 percent compressor fouling (in ISO condition and engine load ratios from 50 to 90%) with data provided in Ref. Mohammadi and Montazeri-Gh (2014) at the same operating conditions. The results are non-dimensional with the corresponding values at the clean compressor conditions. Fig. 8 shows a good compliance between the results provided here and the results of Ref. Mohammadi and Montazeri-Gh (2014). The maximum error occurs in TET parameter which is about 0.38%. Thus, it can be concluded that the compressor fouling is modeled with acceptable accuracy.

5.1.2. Verification of life cycle modeling results of Larson–Miller method

A sample of GG turbine rotor blade life cycle (t_f) distribution computed via finite element method (FEM) is analyzed in this section. The input parameters (turbine stage inlet total pressure and temperature, cooling passage inlet total pressure and temperature, stage outlet static pressure and turbine rotational shaft speed) for this blade life cycle analysis are extracted from the GT modeling code at ISO condition (ambient temperature of 15 °C, ambient barometric pressure of 1.013 bar and relative humidity of 60%) for the GT load ratio of 100%. Then results of the blade conjugate heat transfer analysis (which is used in GT modeling as boundary conditions by the method provided at Section 3) are then imported as boundary and initial conditions into finite element analysis with which finally the blade life analysis is performed. Results show that the minimum value of the blade life cycle occurs at the leading edge and near the blade tip. This is due to increase of turbine cooling air temperature from blade root to tip (as a result of heat transfer with the hot flue gases from blade walls) and consequently higher turbine metal temperature near the blade tip. The same results are reported for the gas turbine blade life cycle analysis in Ref. Eshati et al. (2013).

Prior to initiate the process of creating a data base for training the Neural Network, the results of the blade life cycle analysis are verified at some GT operating points. For this reason, the engine modeling is performed at ISO condition and the blade effective parameters ($\dot{m}_g$, Pg, Tg, $\dot{m}_c$, Pc, Tc, N_{GG}) are computed at GT load ratios from 100 to 105% (which are named D, E, F, G, H engine operating points as presented in Table 3). Then the boundary conditions for the blade life cycle analysis are determined with the use of the mentioned effective parameters. Finally, the blade life cycle are computed at the corresponding operating conditions (by the procedure provided in Section 3) as well as by the method provided in Section 4 (by τ_x curve and Eq. (34)).

Fig. 9 compares the blade life cycle computed by ANSYS (via thermal and stress analyses) at ISO condition and the computed blade life by the use of stress factor curve (Eq. (34)). The above figure shows a good agreement between life cycle analysis using Larson–Miller method and results of stress factor curve (with the average difference of about 9.7%).

5.1.3. Verification of life cycle modeling results by neural network method

After verification of results for rotor blade life cycle analysis (by comparing the blade life cycle results with stress factor curve), rotor blade life cycle was estimated for 811 samples. This procedure is performed by running the GT modeling code for 811 GT operating points including GT load ratio variation from 100 to 105% (ratio of GT load to the GT nominal load, W/Wref), different ambient temperature (from 15 to 45 °C) and also different values of the engine control variables IGV and NGV (IGV from −8 to 36 degrees and NGV from 18 to 27 degrees which was modeled using the method presented at Appendix A). The reason behind using 100 to 105% for GT load ratio range is due to the fact that the mentioned power range is the most critical condition for the turbine blade life cycle which can be estimated based on the engine τ_x curve (Fig. 7). It is worth mentioning that the effects of fouling on life cycle are through the change in input parameters to Neural Network model. Thus GT model provides effective parameters ($\dot{m}_g$, Tg, Pg, $\dot{m}_c$, Tc, Pc, N_{GG}) with existing the fouling effects which will be the input to Neural Network model for estimating the life cycle value.

With knowing the GT model output ($\dot{m}_g$, Pg, Tg, $\dot{m}_c$, Pc, Tc, N_{GG}), the blade temperature distribution and pressure distribution are computed (which are performed via conjugate heat transfer modeling using the method presented at Ref. Alizadeh et al. (2014)). These data are used as boundary conditions of stress and life cycle analyses which finally provided the blade life cycle at 811 operating points.

In the next step, Artificial Neural Network is trained for predicting the blade life cycle as a function of seven above GT effective output parameters which should be entered as the input to Neural Network. In the training procedure, 60% of samples are randomly selected for training and the rest of the samples are evenly used for validation and testing purposes. Also, Multilayer Feed Forward Back Propagation (MFBP) algorithm with one

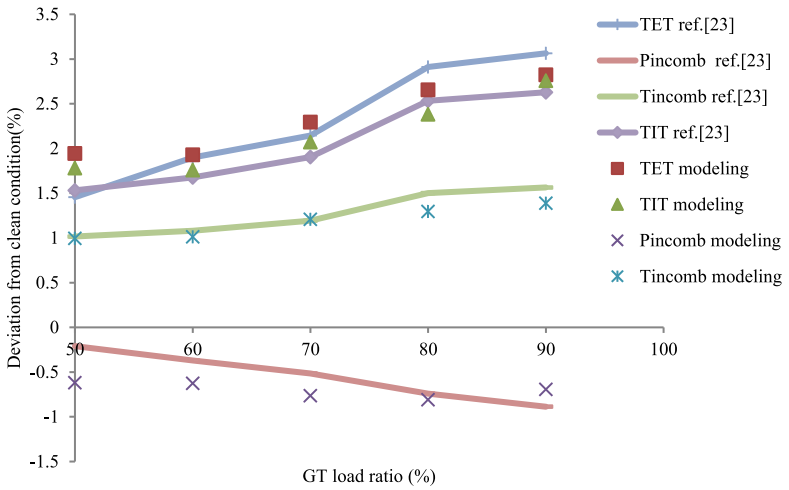

Fig. 8. Comparison of engine modeling results with 7.5% compressor fouling with results reported in Ref. Mohammadi and Montazeri-Gh (2014).

Table 3
Engine modeling results at various load ratios which are used as input parameters for rotor blade life cycle analysis (Fig. 9) at ISO condition and clean compressor.

GT operating points			Effective parameters on turbine blade life cycle						
GT operating points	Wnet (kW)	GT load ratio (%)	$\dot{m}g$ (kg/s)	Tg (°K)	Tc (°K)	$\dot{m}c$ (kg/s)	N_{GG} (rpm)	Pc (bar)	Pg (bar)
D	24 630	100	76.04	1424.14	658.53	3.89	9779.04	14.07	12.2
E	25 122.6	102	76.57	1433.81	661.32	3.92	9821.06	14.21	12.33
F	25 368.9	103	76.71	1441.26	663.52	3.93	9864.87	14.27	12.39
G	25 615.2	104	76.85	1448.52	665.68	3.94	9911.8	14.33	12.45
H	25 861.5	105	77	1455.6	667.82	3.95	9962.32	14.4	12.5

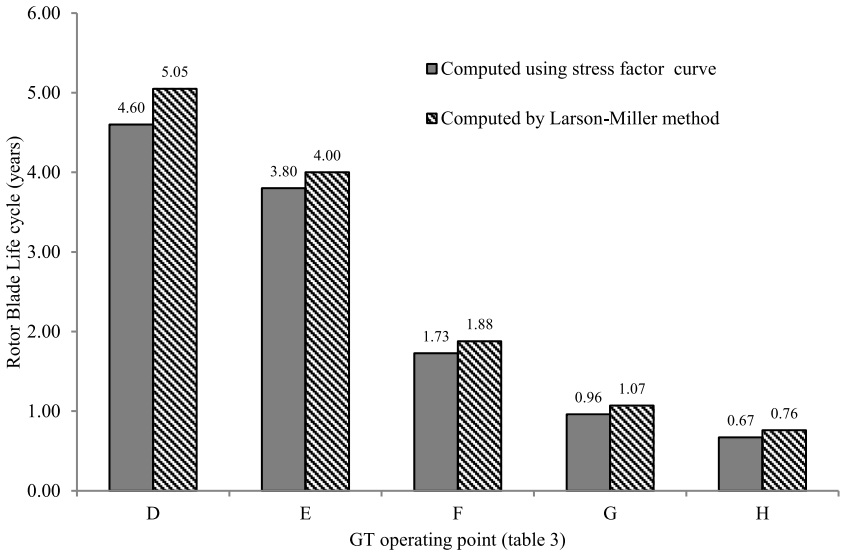

Fig. 9. Comparison of rotor blade life cycle obtained from Larson–Miller method and stress factor with input data at ISO ambient conditions at different GT operating points (for load ratios of 100 to 105% listed in Table 3).

hidden layer (Fig. 6) is selected and number of neurons in the hidden layer is specified. Here, the number of neurons is 14 (twice the number of input parameters) that lead to acceptable accuracy in training process. The input samples for training, testing and validating are selected (by MTLAB) randomly from input data base. The Neural Network training process is repeated until the randomly selected samples cover the entire range of the variation domain for input parameters ($\dot{m}g$, Pg, Tg, $\dot{m}c$, Pc, Tc, N_{GG}) as well as for corresponding output parameter (t_f).

In each epoch (step) of training phase of Neural Network, the coefficients of all vectors connecting input to output parameters become updated until reaching the mean square error (MSE) equal to its acceptable lowest value.

Fig. 10 shows an example of MSE (Eq. (33)) variation with increasing epochs. As per this figure, the training continues until MSE value decreases to an acceptable value (which named the Best point in this figure). MSE of final trained network for estimation of blade creep life cycle is shown in Table 4.

Fig. 11 presents the regression plots of predicted turbine rotor blade life cycle (by the trained neural network) versus the target values (target values are input values for training, testing and validation of the neural network). In these plots Y = T line, expresses the situation that the network results are equal to the

Table 4
MSE for the trained network.

	Blade creep life cycle
MSE for training sample	1.46×10^{-4}
MSE for validation samples	3.96×10^{-4}
MSE for testing samples	4.1×10^{-4}

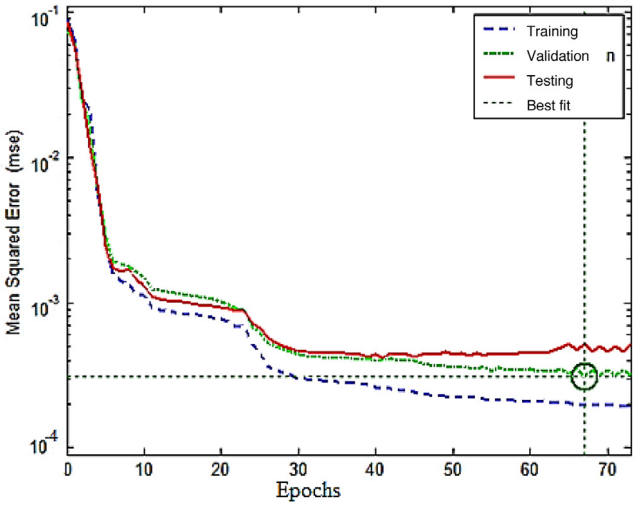

Fig. 10. The computed MSE for the training, validation, and testing. The best fit is for the values of mean squared error (MSE) which shows the convergence of the estimated and existing results for the output.

target values (in the neural network toolbox of MATLAB software the T and Y represent the target output and the neural network produced results respectively). Thus, the more accurate neural network training, the more regression plots are close to Y = T line. This means that in a well-trained neural network, the coefficient of linear regression between neural network outputs and target values is more probably close to 1. From Fig. 11, the average value the coefficients of regression in training, validation and testing phases of the neural network is about 0.99 which proves an acceptable precision of the trained network. Some minor differences between the target values and the results of trained neural network output are observable in Fig. 11. Results showed that neural network output estimation of blade life cycle in comparison with Larson–Miller method had about 4.8% error value in maximum. The mean square error (MSE) value for this comparison was about 10^{-4}

5.2. Modeling results

5.2.1. Effect of ambient temperature on the blade life cycle results

For investigating the effects of ambient temperatures (from 15 to 45 °C) on turbine blade life cycle, the data at GT load ratios from 100 to 105% (the ratio of GT power output to the GT nominal power output at ISO conditions i.e., 24 630 kW) are obtained from the modeling code. Then output parameters such as $\dot{m}$g,Tg, Pg, $\dot{m}$c, Tc, Pc, N_{GG} are introduced into the trained neural network which predicted the turbine blade life cycle for each engine operating point. Fig. 12-d shows the estimated turbine blade life cycle by the neural network for the corresponding input parameters presented in Fig. 12-a to c. These figures show that in a specific GT power output, the blade life cycle reduces exponentially by increasing the ambient temperature due to following reasons:

By increasing the ambient temperature the GT inlet air mass flow rate reduces (due to decreasing the air density), thus for gaining the same engine power output as that for ISO condition, the fuel mass flow rate should be increased which increases the fuel to air ratio as well as turbine inlet gas temperature Tg and turbine blade T_m. Furthermore, increasing the ambient temperature increases the blade cooling air temperature Tc (as is shown in Fig. 12-a) due to increasing compressor inlet and outlet air temperature**s**. It should be mentioned that the turbine blade cooling air is extracted from compressor discharge. Fig. 12-a, shows that the amount of increased Tg and Tc for the engine load ratios of 100%, and ambient temperature variation of 15 to 45 °C are 7.0% and 8.0% respectively.

Another point that can be deduced from Fig. 12-a, is the fact that by increasing the ambient temperature, the turbine inlet gas mass flow rate ($\dot{m}$g) decreases (due to lower compressor inlet air mass flow rate at higher ambient temperatures). Also, the turbine blade coolant mass flow rate decreases by increasing the ambient temperature (T_0) at fixed engine net power output. This is due to decreasing the compressor corrected shaft speed ($N_{GG}/\sqrt{T_0}$) which leads to decreasing the compressor discharged pressure (Pc). With decreasing Pc which is approximately the turbine cooling air supply pressure, the turbine blade cooling air mass flow rate ($\dot{m}$c) reduces. Thus at engine nominal load (load ratio equal to 1.) in the studied ambient temperature range (15 to 45 °C) $\dot{m}$g and $\dot{m}$c change for −5.8% and −7.0% respectively.

The summary of the mentioned effects reduces the turbine blade life cycle severely in GT fixed power output (load ratio from 100% to 105%). To prevent this drawback, the engine control system reduces the net power output by controlling the turbine exit temperature (TET).

At 45 °C ambient temperature, increasing the fuel injection in combustion chamber for providing the nominal load by GT, raises TIT significantly which as Larson–Miller relation predicts, results in decreasing the turbine blade life cycle exponentially.

5.2.2. Effects of change in NGV and IGV values on the blade life cycle results

Change in compressor and turbine geometries (i.e. change in IGV and NGV angles) not only is a method for improving engine key performance parameters such as thermal efficiency and power output (Haglind, 2011), but also it serves as preserving the life cycle of GT hot section parts. In this section the output results of GT modeling for change in NGV and IGV angles (in which NGV varies from 19 to 23° and IGV varies from 17 to 25°) at various GT power output values (load ratios from 90 to 95%) at ambient temperature of 30 °C as input values for the trained Neural network are presented. These operating points are named J to X letters in Table 5. The above mentioned ambient temperatures and GT load ratios are the average values for the studied GT operating conditions in our country. Fig. 13 Shows Neural Network results of life cycle analysis for the above mentioned operating conditions. Fig. 13 shows that at a fixed GT power output, increasing opening of NGV and IGV raises the turbine blade life cycle. This is due to the fact that by increasing NGV opening the power turbine chocking mass flow rate as well as compressor inlet mass flow rate and N_{GG} increase (Appendix A). Rising N_{GG}, results in increase of compressor pressure ratio (PR_{comp}) as well as raise in both turbine blade air cooling pressure (P_c) and air cooling mass flow rate ($\dot{m}$c). Furthermore, increasing $\dot{m}_{in,comp}$ decreases the fuel to air mass flow rate ratio and turbine inlet gas temperature (decreasing Tg as is shown in Table 5). The reason for this observation as mentioned before is that at a fixed GT power output when NGV opens (increases) the turbine chocking mass flow rate increases. This results in increasing the compressor inlet mass flow rate and N_{GG}. Rising N_{GG}, results in increase of compressor pressure ratio (PR_{comp}) as well as rise in both Pc and $\dot{m}$c.

The above mentioned effects lead to reduction in turbine blade metal temperature.

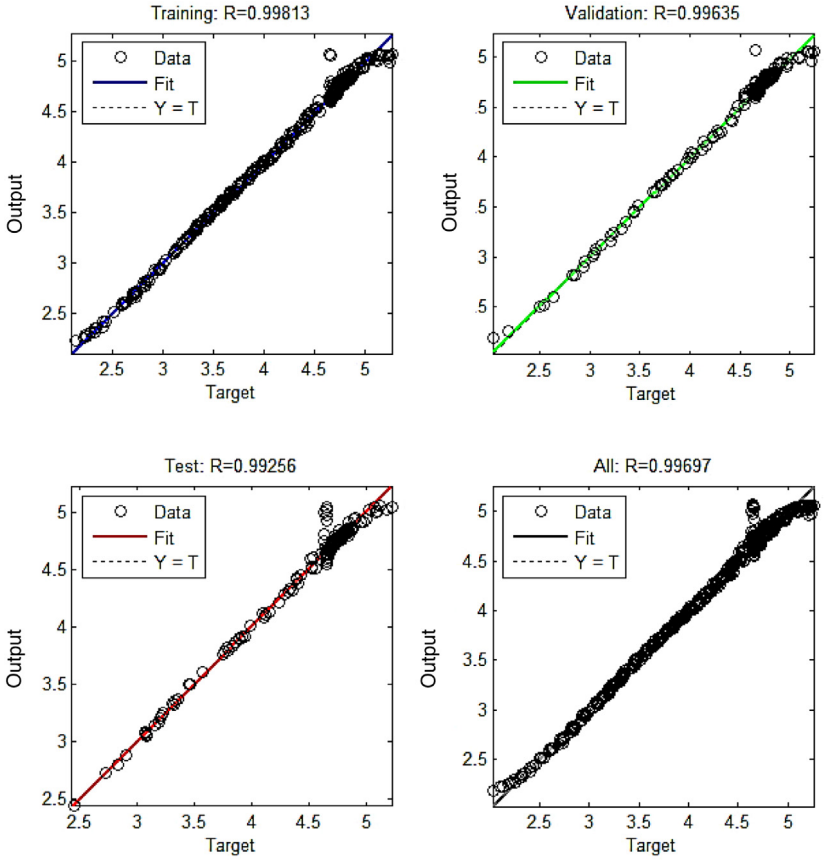

Fig. 11. Regression plots of predicted turbine rotor blade life cycle versus the target values (obtained from Larson–Miller method).

Table 5
Engine modeling results at various load ratios as well as various NGV and IGV values which are used as input parameters to neural network trained model for rotor blade life cycle estimation (Fig. 9) at 30 °C of ambient temperature and clean compressor and GT load ratio from 90 to 95%.

GT operating points	GT net power (kW)	GT load ratio (%)	NGV (degree)	IGV (degree)	$\dot{m}g$ (kg/s)	Tg (°K)	Tc (°K)	$\dot{m}c$ (kg/s)	N_{GG} (rpm)	Pc (bar)	Pg (bar)	TET–TET_design
J	22 167	90	23	22	72.17	1430	681	3.65	9676	13.4	11.6	12.88
K	22 462.6	91	23	23	72.53	1435	682	3.67	9695	13.5	11.7	15.26
L	22 758.1	92	23	24	72.88	1440	684	3.69	9713	13.6	11.8	17.57
M	23 053.7	94	23	24	73.24	1446	685	3.71	9731	13.7	11.9	19.88
N	23 349.2	95	23	25	73.59	1451	687	3.73	9749	13.8	11.9	22.16
O	22 167	90	21	19	70.52	1437	675	3.59	9591	13.1	11.4	19.84
P	22 462.6	91	21	20	70.88	1442	677	3.61	9607	13.2	11.5	21.99
Q	22 758.1	92	21	21	71.23	1448	678	3.63	9626	13.3	11.5	24.25
R	23 053.7	94	21	21	71.58	1453	680	3.65	9645	13.4	11.6	26.51
S	23 349.2	95	21	22	71.93	1458	681	3.67	9663	13.5	11.7	28.77
T	22 167	90	19	17	68.74	1448	670	3.52	9517	12.8	11.1	29.12
U	22 462.6	91	19	17	69.09	1453	671	3.53	9531	12.9	11.2	31.28
V	22 758.1	92	19	18	69.43	1458	673	3.55	9546	13	11.3	33.5
W	23 053.7	94	19	18	69.78	1463	674	3.57	9560	13.1	11.4	35.71
X	23 349.2	95	19	19	70.12	1469	675	3.59	9574	13.2	11.4	37.89

By reducing the turbine blade metal temperature the turbine blade life cycle rises (Eq. (26)).

For example in GT power output of 22 167 kW, opening the NGV/IGV from 17°/19° to 22°/23° improves the turbine blade life from 1.96 to 3.03 years which is mainly caused by reducing Tg from 1448 to 1430 °K and increasing the turbine cooling air mass flow ($\dot{m}c$) from 3.52 to 3.65 kg/s (Table 5).

5.2.3. Effect of compressor fouling on life cycle results

In addition to variation of the ambient temperature, the GT component faults such as compressor and turbine fouling may affect the turbine blade life cycle. The mentioned problems change the engine performance parameters (such as compressor and turbine efficiency, compressor inlet mass flow rate, turbine inlet temperature and etc.) which results in turbine blade life cycle variation. The fouling effects on the engine performance parameters are studied in Mohammadi and Montazeri-Gh (2014), but in this paper the fouling effects on both GT operating parameters and the turbine blade life cycle are investigated.

In this section the effects of compressor fouling on the turbine blade life cycle is investigated. Thus, the amount of compressor fouling is entered to the engine modeling code (using the method provided at Section 2) which enables modeling gas turbine even when its compressor is fouled. Then the effective parameters on the blade life cycle ($\dot{m}g$, Tg, Pg, $\dot{m}c$, Tc, Pc, N_{GG}) are computed by running the gas turbine model including the fouled compressor.

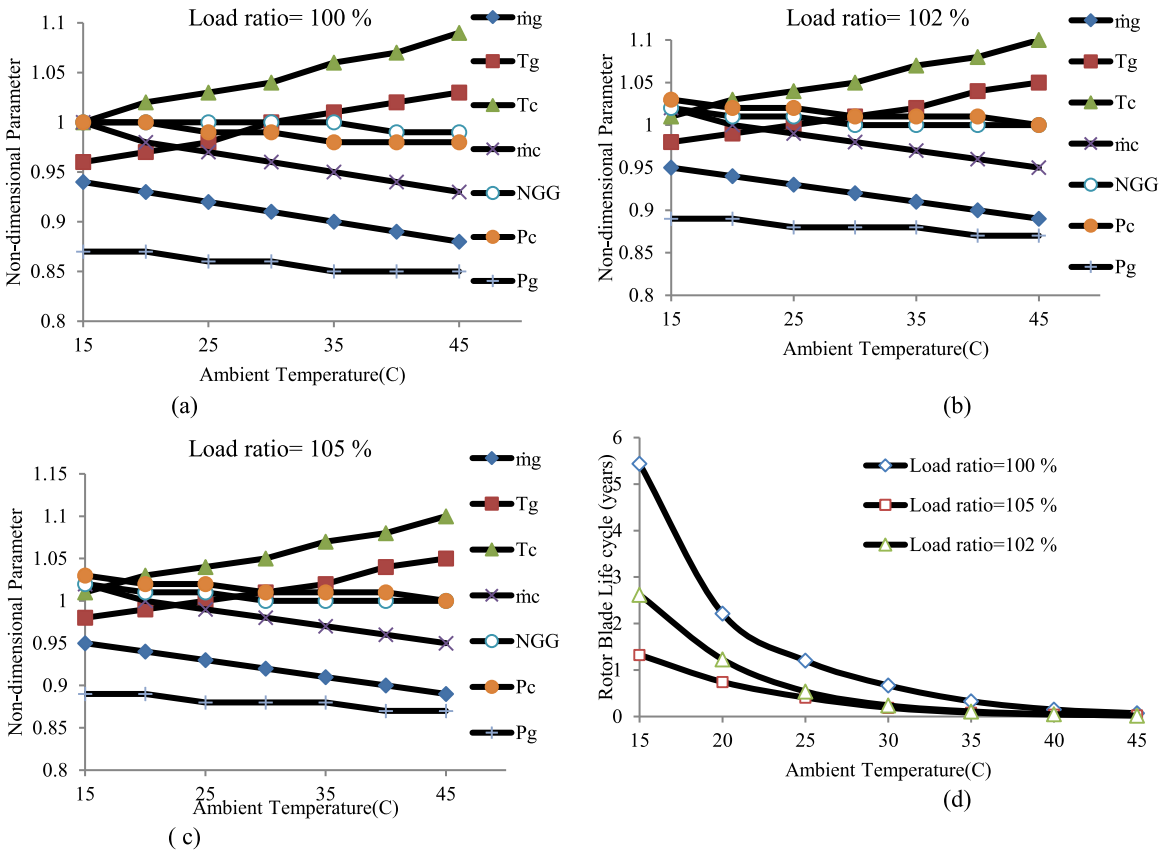

Fig. 12. Rotor blade life at different ambient temperatures and different GT load ratios.

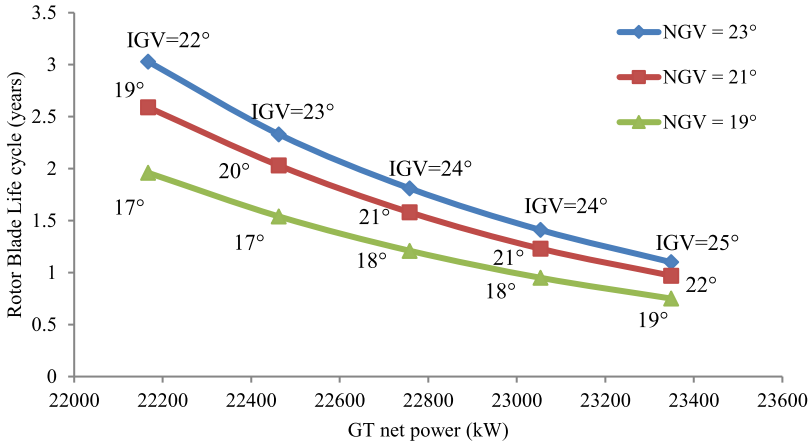

Fig. 13. Rotor blade life cycle obtained from neural network model which is trained for various NGV and IGV values and other input parameters (listed in Table 5) at ambient temperature of 30 °C.

The range of change in compressor fouling is 0 to 7.5%. Then the GT modeling output is used as input for the trained neural network to estimate the blade life cycle.

Fig. 14-d presents the turbine blade life cycle at different compressor fouling levels in an engine running at 100% load ratio and various ambient temperatures. As Fig. 14-d shows, in a specific engine load and ambient temperature, increasing the compressor fouling percent leads to decrease the turbine blade life cycle sharply. This is due to decreasing the compressor inlet air mass flow rate with increasing the compressor fouling (Section 2).

Furthermore in this situation the discharge pressure (Pc) decreases. This is due to shifting the engine operating point on the compressor map from clean to fouled condition as is shown in Fig. 3. This figure illustrates that for an approximate fixed non-dimensional compressor corrected speed (defined in Section 2), compressor discharged corrected pressure ratio and corrected mass flow rate reduce. Fig. 14-a to c show that with increasing the fouling percent up to 7.5% at various ambient temperatures, the increase in N_{GG} is small and for 15 °C ambient temperature (Fig. 14-a), N_{GG} variation is just about 1.5%. With decreasing the Pc value the turbine blade cooling air mass flow rate ($\dot{m}c$) drops. This is due to the fact that the turbine blade cooling air is extracted from the compressor discharged air and thus decreasing the Pc, decreases the turbine cooling air supply pressure. For

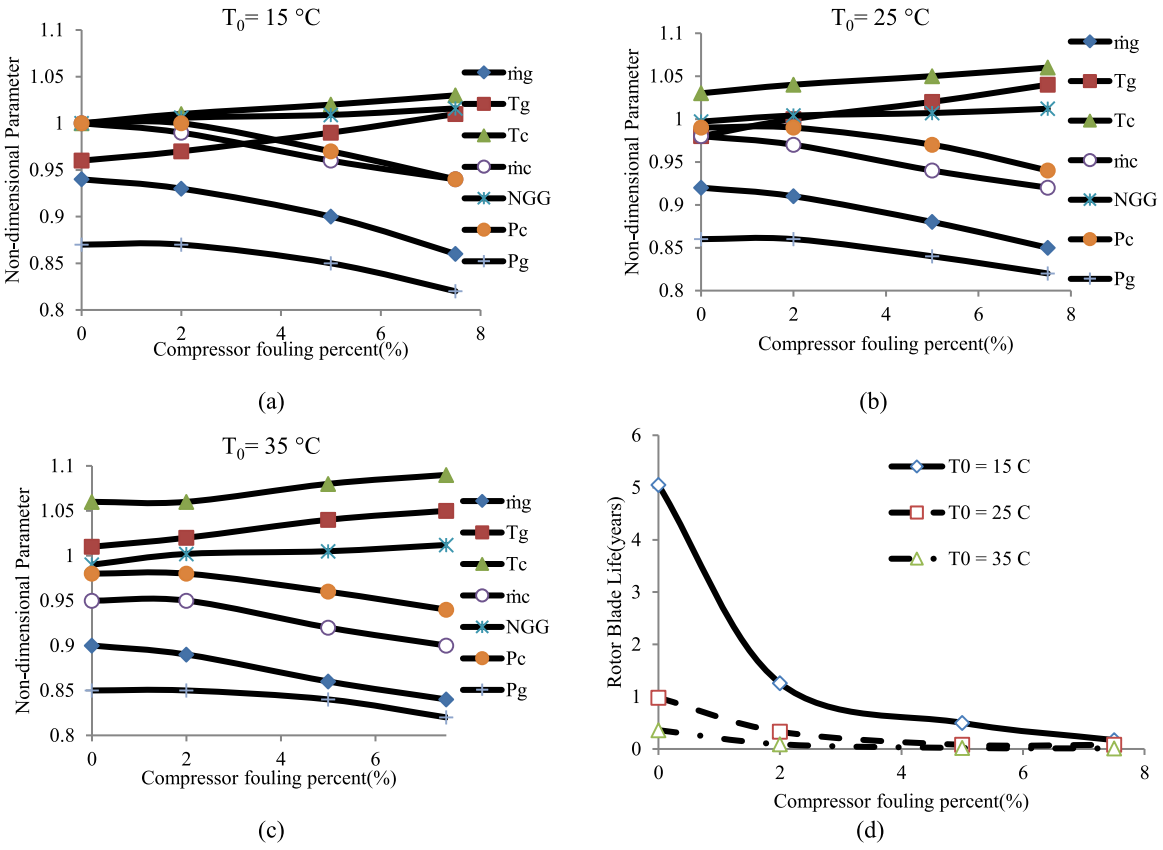

Fig. 14. Rotor blade life cycle at different compressor fouling percent values at GT load ratio of 100% and different ambient temperatures.

instance in the ambient temperature of 15 °C, both Pc and $\dot{m}c$ reduce for 6% (relative to the clean condition).

Moreover, the turbine blade cooling air temperature (Tc) rises when the compressor fouling increases. Results show that for the compressor fouling of 7.5%, Tc increases by 3.0%. Increase in Tc is due to increasing the compressor shaft speed (N_{GG}) and also decreasing compressor efficiency in the compressor fouled condition. Decreasing the compressor isentropic efficiency also leads to more entropy generation in air compression process in compressor and consequently boosts the compressor discharge air temperature.

The mentioned effects increase the turbine metal temperature (caused by increasing the $\dot{m}g$, Tg and reduced $\dot{m}c$) and also increase centrifugal stress in the turbine blade (caused by increase in NGG) which finally reduces the turbine blade life cycle (Eq. (26)).

It should be noted that in real life and at the above conditions the fuel mass flow rate decreases to maintain the required life time of the engine hot parts (mainly the first GG turbine rotor blades). Thus the GT power output at base load condition decreases (by limiting the fuel mass flow rate) from 24 600 kW to a lower value at high ambient temperatures or compressor fouling condition. In this situation if the engine runs to produce nominal power output, the operating conditions damages the rotor blades.

Therefore it can be concluded that the compressor fouling has a profound effect on the life cycle of the engine hot section parts, this effect is mainly due to increasing the engine firing temperature (Tg). The reason is decreasing compressor inlet air mass flow rate and consequently increasing fuel to air ratio for reaching the same specific GT power output when compressor is not fouled. At this situation with cooling air mass flow reduction, the turbine cooling air temperature also rises.

6. Conclusion

Industrial gas turbine first rotor blade life cycle analysis is performed at the engine base or peak load conditions and 15 to 45 °C ambient temperatures. Then the blade life cycle analysis is performed for various GT operating conditions including change in the ambient temperature, compressor and turbine geometries (different IGV and NGV angles), as well as various load ratios (which produced 811 samples of blade life cycle analysis). Based on the blade thermal and stress analysis, the blade life cycle was assumed to be a function of some key engine operating parameters ($\dot{m}g$, Tg, Pg, $\dot{m}c$, Tc, Pc, N_{GG}). These parameters mainly affect the convective heat transfer coefficients in the blade inside and outside surfaces and in this way change the blade metal temperature together with thermo-mechanical stresses in the blade walls which finally affect the blade life cycle (as Larson–Miller relation Eq. (26) shows). These parameters are normalized and used for training a neural network. This is performed using Multi-layer Feed forward Back Propagation (MFBP) algorithm with mean square error of about 10^{-4}. The results of the blade life cycle analysis obtained from GT modeling as well as thermal and stress analyses are compared with the engine manufacturer stress factor curve. Results show that for the GT nominal and peak loads, the estimated blade life cycle is in good agreement with the creep factor curve results (with an average error of 9.7%). Then the effects of GT operating and health conditions (such as different ambient temperatures, various IGV and NGV angles, various GT load ratios and also different compressor fouling percent values) on the blade life cycle are studied using the trained neural network. Results show that in a specified GT load ratio and by increasing the ambient air temperature, or by increasing the compressor fouling percent, the rotor blade life cycle decreases exponentially (as Larson–Miller relation Eq. (26)

predicts). For example in ambient temperature range of 15 to 45 °C and GT load ratios of 100% to 105%, the GG turbine first rotor blade life cycle reduces from 4.85 to 0.07 years if we expect to get the same power output as that for ISO ambient condition. Similarly due to the compressor fouling, the life cycle changes in range of 0 to 7.5% at ambient temperature of 15 °C and for engine load ratio of 100%, the turbine blade life cycle varied from 4.85 to 0.68 years if we expect to get the same power output as that for clean condition. These results are obtained by the trained neural network model. The model can be also used for conditional monitoring, maintenance and operation to prevent the unexpected engine failure and unplanned engine shut down.

Declaration of competing interest

The authors declare that they have no known competing financial interests or personal relationships that could have appeared to influence the work reported in this paper.

Acknowledgment

The authors would like to thank Turbotec Co. for providing data for comparison and validation of our modeling results. Also, the authors declare that there is no conflict of interest in preparing and presentation of this manuscript.

Appendix A. Variable geometry compressor modeling (using compressor map scaling)

The variable geometry compressor modeling was done using the linear map scaling method (Bringhenti and Barbosa, 2004; Haglind, 2010; Kim and Hwang, 2006; Silva et al., 2005). In this method the variation of the compressor inlet mass flow rate, pressure ratio and isentropic efficiency (at each specific rotational speed) as function of changing the compressor inlet guide vane angle (i.e. IGV) were formulated as following relations:

$$\dot{M}_{in,comp,cor} = \dot{M}_{in,comp}\left(1 + \frac{c_1 \times \Delta\gamma_{IGV}}{100}\right) \tag{A.1}$$

$$\pi_{comp,cor} = \pi_{comp}\left(1 + \frac{c_2 \times \Delta\gamma_{IGV}}{100}\right) \tag{A.2}$$

$$\eta_{comp,cor} = \eta_{comp}\left(1 - \frac{c_3 \times \Delta\gamma_{IGV}}{100}\right) \tag{A.3}$$

where $\Delta\gamma_{IGV}$, is the variation in IGV angle. In another word, the compressor map of a GT engine has different non-dimensional corrected compressor shaft speed lines $\left(N_{GG}/\sqrt{T_{in,GG}}/\left(N_{GG}/\sqrt{T_{in,GG}}\right)_{design}\right)$ and each speed line associates with a specific IGV opening angle named $IGV_{selected}$. To take into account the effects of change of IGV opening angles in compressor map and to perform GT modeling as well as turbine blade life analysis, some small step variations about each $IGV_{selected}$ angle (for each specific compressor speed line) are considered. Then $\Delta\gamma_{IGV}$, which is the difference between IGV_{step} and $IGV_{selected}$ is defined as:

$$\Delta\gamma_{IGV} = IGV_{step} - IGV_{selected} \tag{A.4}$$

Moreover, c_1, c_2 and c_3 are constant coefficients which were obtained from analysis of CFD results for compressor maps at different IGV opening angle (using the CFD setup provided in Rashidzadeh et al. (2015) for the studied engine CFD analysis). Fig. A.1 compares the compressor maps for three different $\Delta\gamma_{IGV}$ values ($\Delta\gamma_{IGV} = -3, 0, +3$). In this figure the air flow direction is shown and the maximum $IGV_{selected}$ opening (i.e., maximum air flow frontal area) occurs at angle $+36°$ and minimum $IGV_{selected}$ opening (i.e., minimum air flow frontal area) occurs at $-8°$.

Variable turbine geometry (NGV) modeling

The same procedure as the compressor variable geometry modeling was implemented for modeling the turbine variable geometry. The variation of the power turbine inlet mass flow rate and isentropic efficiency were formulated as a function of the changing the power turbine nozzle guide vane angle (Eqs. (A.5) and (A.6)):

$$\dot{M}_{in,turb,cor} = \dot{M}_{in,turb}\left(1 - \frac{c_4 \times \Delta\gamma_{NGV}}{100}\right) \tag{A.5}$$

$$\eta_{turb,cor} = \eta_{turb}\left(1 + \frac{c_5 \times \Delta\gamma_{NGV}}{100}\right) \tag{A.6}$$

where $\Delta\gamma_{NGV}$ is change in power turbine inlet nozzle vane angle and c_4., c_5 are constant coefficients which were obtained from analysis of CFD results for PT turbine first stage and various NGV angles(using the CFD set up that presented at Rashidzadeh et al. (2015) for the studied engine CFD analysis). Fig. A.2 presents the power turbine first stage characteristic map for different inlet nozzle vane angles. This figure shows that the selected opening angle of NGV relative to the turbine shaft axis (in the studied engine) is 21° degrees. With decreasing and increasing of opening angle at different steps ($\Delta\gamma_{NGV} = NGV_{step} - NGV_{selected} = NGV_{step} - 21$) the turbine map shifts up and down. In this figure the flue gas flow direction is shown and the maximum NGV opening (i.e., maximum flue gas flow frontal area) occurs at angle $+27°$ and minimum NGV opening (i.e., minimum flue gas flow frontal area) occurs at 18°.

Appendix B. Gas compressor (GC) modeling

When the gas turbine is used as a driver for natural gas compression, it is named turbo-compressor. In this case the GT power output will be used for running gas compressor (GC) and provide GC power consumption. Input parameters for GC modeling are GC pressure ratio (the ratio of natural gas compressor station outlet to inlet pressure) as well as natural gas inlet pressure and temperature. At the first step, the GC shaft rotational speed is guessed and then the GC inlet gas mass flow rate and isentropic efficiency are computed using the characteristic maps:

$$\dot{M}_{in,comp,GC}(\pi_{comp,GC}, NPT) = c_1(NPT)\pi^3_{comp,GC} + c_2(NPT)\pi^2_{comp,GC} + c_3(NPT)\pi_{comp,GC} + c_4(NPT) \tag{B.1}$$

$$c_i = c_{i1}NPT^3 + c_{i2}NPT^2 + c_{i3}NPT + c_{i4} \tag{B.2}$$

$$\eta_{comp,GC}(\pi_{comp,GC}, NPT) = b_1(NPT)\pi^3_{comp,GC} + b_2(NPT)\pi^2_{comp,GC} + b_3(NPT)\pi_{comp,GC} + b_4(NPT) \tag{B.3}$$

$$b_i = b_{i1}NPT^3 + b_{i2}NPT^2 + b_{i3}NPT + b_{i4} \tag{B.4}$$

In the above equations $\pi_{comp,GC}$, NPT are GC pressure ratio and PT (or GC shaft) rotational speed respectively. Also, c_{i1}, c_{i2}, c_{i3}, c_{i4} are the coefficients of the GC map (mass flow rate vs. pressure ratio map) which are obtained by third order curve fitting. b_{i1}, b_{i2}, b_{i3}, b_{i4} are also coefficients of third order curve fitting for GC map. After computing the GC inlet mass flow rate and isentropic efficiency, the absorbed power was computed from Eqs. (B.5) and (B.6).

$$T_{ex,comp,GC} = T_{in,comp,GC}\left[1 + \frac{1}{\eta_{comp,GC}}\left(PR^{\frac{\gamma-1}{\gamma}}_{comp,GC} - 1\right)\right] \tag{B.5}$$

$$W_{comp,GC} = \dot{m}_{in,comp,GC} \times C_{p,g} \times (T_{ex,comp,GC} - T_{in,comp,GC}) \tag{B.6}$$

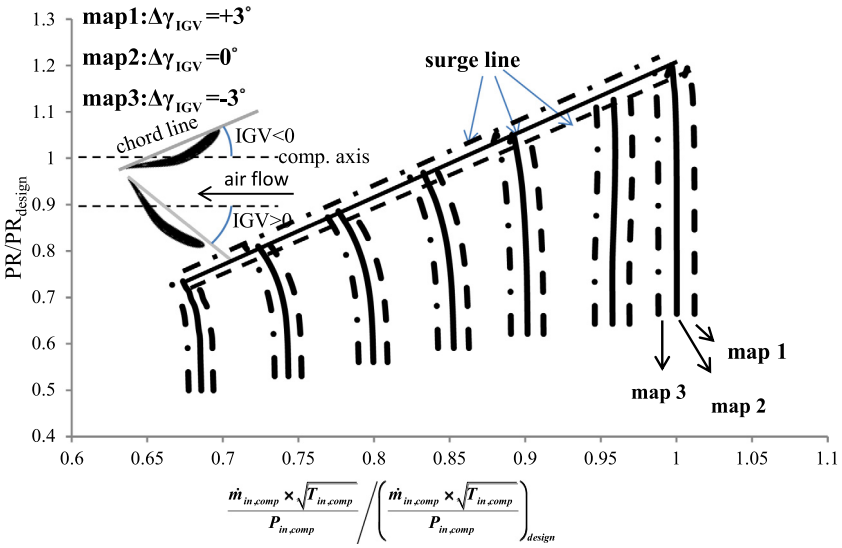

Fig. A.1. Compressor map at different IGV values.

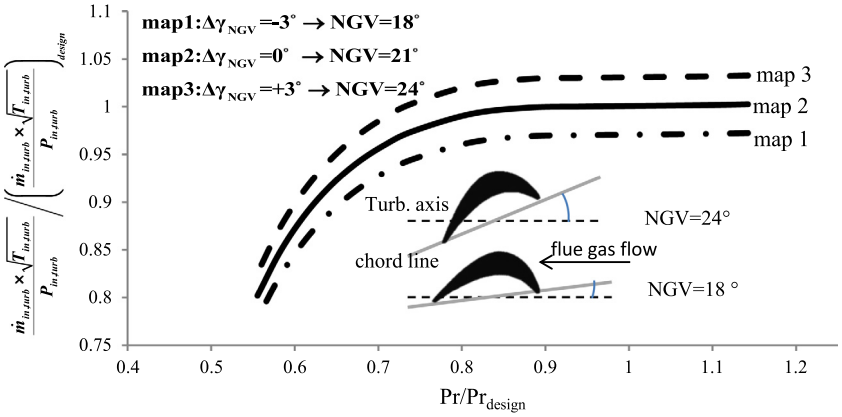

Fig. A.2. PT fist stage map at different NGV values.

Another auxiliary equation was equality of GC absorbed power and power output of PT turbine which was solved in the system of governing equations for the whole turbo compressor assembly (Eqs. (B.1) to (B.6)). Newton–Raphson algorithm corrects the PT rotational speed in try and error scheme to fulfill the auxiliary equation.

References

Abdul Ghafir, M.F., Li, Y.G., Singh, R., Huang, K., Feng, X., 2010. Impact of operating and health conditions on aero gas turbine: Hot section creep life using a creep factor approach. (43987), 533–545.

Alizadeh, M., Izadi, A., Fathi, A., 2014. Sensitivity analysis on turbine blade temperature distribution using conjugate heat transfer simulation. J. Turbomach. 136 (1), 011001.

Ben-Israel, A., 1966. A Newton–Raphson method for the solution of systems of equations. J. Math. Anal. Appl. 15 (2), 243–252.

Bringhenti, C., Barbosa, J., 2004. Methodology for gas turbine performance improvement using variable-geometry compressors and turbines. Proc. Inst. Mech. Eng. A 218 (7), 541–549, %@ 0957-6509.

Camporeale, S., Fortunato, B., Mastrovito, M., 2006. A modular code for real time dynamic simulation of gas turbines in simulink. J. Eng. Gas Turbines Power 128 (3), 506–517.

Deuflhard, P., 1974. A modified Newton method for the solution of ill-conditioned systems of nonlinear equations with application to multiple shooting. Numer. Math. 22 (4), 289–315.

El-Masri, M., 1988. GASCAN—an interactive code for thermal analysis of gas turbine systems. J. Eng. Gas Turbines Power 110 (2), 201–209.

Eshati, S., 2012. An Evaluation of Operation and Creep Life of Stationary Gas Turbine Engine (Ph.D. thesis). Cranfield University.

Eshati, S., Abu, A., Laskaridis, P., Khan, V., 2013. Influence of water–air ratio on the heat transfer and creep life of a high pressure gas turbine blade. Appl. Therm. Eng. 60 (1), 335–347.

Evans, R.W., Wilshire, Brian, 1993. Introduction to Creep. The Institute of Materials(UK), p. 115.

Fouflias, D., Gannan, A., Ramsden, K., Pilidis, P., Mba, D., Teixeira, J., Igie, U., Lambart, P., 2010. Experimental investigation of the influence of fouling on compressor cascade characteristics and implications for gas turbine engine performance. Proc. Inst. Mech. Eng. A 224 (7), 1007–1018.

Ghafir, M.A., Li, Y.G., Wang, L., 2014. Creep life prediction for aero gas turbine hot section component using artificial neural networks. J. Eng. Gas Turbines Power 136 (3), 031504.

Haglind, F., 2010. Variable geometry gas turbines for improving the part-load performance of marine combined cycles–Gas turbine performance. Energy 35 (2), 562–570.

Haglind, F., 2011. Variable geometry gas turbines for improving the part-load performance of marine combined cycles–Combined cycle performance. Appl. Therm. Eng. 31 (4), 467–476, %@ 1359-4311.

Hay, N., Taylor, J.H., 1984. Effect of reducing the blade cooling air temperature and mass flow on blade life and cycle efficiency. Proc. Inst. Mech. Eng. A 198 (3), 225–230.

Haykin, S.S., 2001. Neural Networks: A Comprehensive Foundation. Tsinghua University Press.

ISO 3977-9 Internal Standard, 1999. Gas turbine, Procurement, Part 9: Reliability, availability, maintainability and safety.

Kim, T.S., Hwang, S.H., 2006. Part load performance analysis of recuperated gas turbines considering engine configuration and operation strategy. Energy 31 (2–3), 260–277.

Kim, J., Kim, T.S., Lee, J.S., Ro, S.T., 1996. Performance analysis of a turbine stage having cooled nozzle blades with trailing edge ejection. Am. Soc. Mech. Eng. (Paper) 1–8.

Li, Y., Nilkitsaranont, P., 2009. Gas turbine performance prognostic for condition-based maintenance. Appl. Energy 86 (10), 2152–2161.
Marahleh, G., Kheder, A., Hamad, H., 2006. Creep-life prediction of service-exposed turbine blades. Mater. Sci. 42 (4), 476.
Meitner, P.L., 1990. Computer code for predicting coolant flow and heat transfer in turbomachinery.
Mino, K., et al., 2001. Residual life prediction of turbine blades of aeroderivative gas turbines. Adv. Eng. Mater. 3 (11), 922.
Mohammadi, E., Montazeri-Gh, M., 2014. Simulation of full and part-load performance deterioration of industrial two-shaft gas turbine. J. Eng. Gas Turbines Power 136 (9), 092602.
Nyberg, Ingela, Continued Product Development /Possibilities SGT-600/700 Part 1. Siemens Industrial Turbomachinery.
Parthasarathy, G., Menon, S., Richardson, K., Jameel, A., McNamee, D., Desper, T., Gorelik, M., Hickenbottom, C., 2008. Neural network models for usage based remaining life computation. J. Eng. Gas Turbines Power 130 (1), 012508–012508–7.
Rashidzadeh, H., Hosseinalipour, S.M., Mohammadzadeh, A., 2015. The SGT-600 industrial twin-shaft gas turbine modeling for mechanical drive applications at the steady state conditions. J. Mech. Sci. Technol. 29 (10), 4473–4481.
Rinman, J., Maintenance Pan SGT-600 Mechanical Drive, Siemens Industrial Turbomachinery.
Rumelhart, D.E., Hinton, Geoffrey, E., Williams, Ronald, J., 1985. Learning Internal Representations by Error Propagation. California Univ San Diego La Jolla Inst for Cognitive Science.
Sanjay, Singh, O., Prasad, B.N., 2009. Comparative evaluation of gas turbine power plant performance for different blade cooling means. Proc. Inst. Mech. Eng. A 223 (1), 71–82.
Siemens, 2006. Maitenance plan SGT-600/GT10A/B1/B2. p. 8(11).
Silva, V.V.R., Khatib, W.F., Peter, J., 2005. Performance optimization of gas turbine engine. Eng. Appl. Artif. Intell. 18 (5), 575–583, %@ 0952-1976.
Tahan, et al., 2017. Performance-based health monitoring, diagnostics and prognostics for condition-based maintenance of gas turbines: A review. Appl. Energy 198, 122–144.
Vaezi, M., Soleymani, M., 2009. Creep life prediction of inconel 738 gas turbine blade. J. Appl. Sci. 9 (10), 1950–1955.
VanWylen, G., Borgnakke, C., Sonntag, R.E., 1998. Fundamentals of Classical Thermodynamics. John Wiley & Sons.
Wood, M., 2000. Gas turbine hot section components: the challenge of ‘residual life’assessment. Proc. Inst. Mech. Eng. A 214 (3), 193–201.
Zaretsky, E.V., Litt, Jonathan S., Hendricks, Robert C., Soditus, Sherry M., 2012. Determination of turbine blade life from engine field data. J. Propul. Power 28 (6), 1156–1167.